Journal of Geochemical Exploration 185 (2018) 33–51

Contents lists available at ScienceDirect

Journal of Geochemical Exploration

journal homepage: www.elsevier.com/locate/gexplo

Sources, enrichment, and redistribution of As, Cd, Cu, Li, Mo, and Sb in the Northern Atacama Region, Chile: Implications for arid watersheds affected by mining

Tapia J.[a,*], Davenport J.[b], Townley B.[c], Dorador C.[d], Schneider B.[e], Tolorza V.[a], von Tümpling W.[f]

[a] Instituto de Ciencias de la Tierra, Facultad de Ciencias, Universidad Austral de Chile, Chile
[b] Université de Lorraine CNRS-CRPG, Vandœuvre-lés-Nancy, France
[c] Departamento de Geología y Advanced Mining Technology Center, Facultad de Ciencias Físicas y Matemáticas, Universidad de Chile, Chile
[d] Departamento de Biotecnología, Facultad de Ciencias del Mar y Recursos Biológicos e Instituto Antofagasta, Universidad de Antofagasta, Chile
[e] Montgomery & Associates, Vitacura 2771, Las Condes, Santiago, Chile
[f] Helmholtz Centre for Environmental Research – UFZ, Central Laboratory for Water Analytics & Chemometrics, Brückstrasse 3a, 39114 Magdeburg, Germany

ABSTRACT

Long-established and widespread mining activities in the Northern Atacama Region of Chile have historically impacted the environment. Most notably, the Potrerillos and El Salvador mines, until 1976, were responsible for dumping over $150 \cdot 10^6$ tons of tailings into the El Salado River, discharging directly into the bay of Chañaral on the coast. Water resources in the Northern Atacama Region are scarce; the few include the El Salado River and the Pedernales, Maricunga, and Laguna Verde basins. This region also contains two highly sensitive national parks: the Pan de Azúcar on the coast and the Nevado de Tres Cruces in the Andes.

Protecting available water resources in this inherently dry region is critical and environmental degradation that has occurred has not been reported in terms of the most important superficial pollutants. In order to specifically evaluate the metals and metalloids polluting superficial water and fluvial sediments, a 3 year-long survey was carried out in the basins of the Northern Atacama Region. Additionally, impacts of the El Salado River flood in March 2015 were evaluated.

When compared to the average concentrations of dissolved elements in river water worldwide, the most enriched elements of the Northern Atacama Region are, in decreasing order: Li, As, Mo, ± Cd, Sb, and Cu. In the case of fluvial sediments, compared to the composition of the upper continental crust, samples are enriched in the following elements (in decreasing order): As, Cu, Mo, Li, ± Cd and Sb. In surface waters, dissolved As, Li, Mo and Cd are naturally enriched, concentrations of Cu and Sb are inferred to be related to mining activities. In fluvial sediments, concentrations of As, Li and Cd are of natural origin while Cu, Mo and Sb are related to the exploitation and mineral treatment of porphyry copper deposits.

During the intense March 2015 flood event, contaminant elements were remobilized in the Andes Mountains and El Salado Alto Basin, and concentrations increased in the El Salado Bajo Basin predominantly due to the creation of a hydrologic connection between adjacent basins. Despite the presence of world-class porphyry Cu-Mo and iron oxide copper-gold deposits in the region, some of which have been mined since the end of the 19th century, concentrations of dissolved Cu are lower than previously reported. This is likely related to circumneutral pH and the complexation of Cu as a cation in contrast to As and Mo which might be stable as $HAsO_4^{2-}$ and MoO_4^{2-}, respectively, in solution over long distances.

1. Introduction

The Northern Atacama Region of Chile, specifically located between 26 and 27°S, is one of the most inhospitable places in the Atacama Desert. Despite arid to hyper arid conditions since the Late Triassic (Clarke, 2006), there are a few available water resources. Sources of extractable groundwater include the El Salado, Pedernales, Maricunga, and Laguna Verde basins, in which two highly sensitive National Parks exist, the Nevado Tres Cruces in the Andes (Earle et al., 2003) and the Pan de Azúcar on the coast (Thompson et al., 2003). The El Salado

* Corresponding author.
E-mail address: joseline.tapia@uach.cl (J. Tapia).

https://doi.org/10.1016/j.gexplo.2017.10.021
Received 17 May 2017; Received in revised form 6 October 2017; Accepted 26 October 2017
Available online 31 October 2017
0375-6742/

River drains into the Pacific Ocean and is the only superficial water system in the Northern Atacama Region. In particular, groundwater is a valuable resource that is supplied predominantly by precipitation and surface water infiltration; aside from potable water use, it is estimated that 70% of extracted groundwater is utilized for mining operations (Neary and García-Chevesich, 2008).

The Northern Atacama Region also hosts important mineral deposits. Since 1894, the seams and veins of the El Salvador porphyry copper deposit, in the Potrerillos district, were mined by selective methods followed by block caving methods (Olson, 1989). More recently, other deposit types explored and exploited in this region consist of stratabound (Espinoza, 1990), iron oxide copper-gold (IOCG) and iron oxide-apatite (IOA) deposits along the Coastal Cordillera (Benavides et al., 2007) as well as epithermal Cu-Au deposits in the Andes (Sillitoe, 1997). Additionally, Li has become an important commodity, especially in the Pedernales and Maricunga salt flats (Gajardo, 2014). As a result of the economic potential and large-scale mining efforts, the El Salado River has been affected by intense and often uncontrolled mining activities during the 20th and 21st century (Ramírez et al., 2005).

To date, no geochemical baseline analysis has been conducted for contaminants in surface water and fluvial sediments in the Northern Atacama Region of Chile, in non-storm conditions or as a function of storm events which are infrequent but powerful in regard to their impacts on inhabitants of the region and the environment (i.e. flooding and distribution of water sources). A comprehensive understanding of contaminant sources, in addition to their distribution and redistribution, is critical in the Atacama Desert due to water scarcity and the importance of sustaining current ecosystems. In the case of groundwater that is recharged by surface water such as the El Salado River, its quality impacts consumption and utilization for mining as the concentrations of contaminants such as As in water affect the production and processing of copper concentrate (International Mining, 2016). In addition, although infrequent, flood events can potentially create a connection between areas of the region not normally linked hydrologically. This connection, which forms as a function of higher water levels in upgradient areas, can act as a conduit for the flow and transport of potential contaminants to areas downgradient where such species may not be present under normal, non-storm conditions.

Through conducting a 3-year long survey of surface water and fluvial sediments in the Northern Atacama Region, this study aims to: (i) identify and evaluate the main contaminants and probable sources, (ii) establish a local geochemical background of the naturally and otherwise anthropogenically enriched elements in surface water and fluvial sediments, and (iii) document the influence of the March 2015 storm event and mudflow in the Northern Atacama Region on the redistribution of contaminant elements. In regard to the flooding of the El Salado River which caused the March 2015 mudflow, metallic contaminants of surface water and fluvial sediments in the region were characterized and compared before, two months after, and one year after the event. As such, the presented results, discussions, and conclusions can have broader implications in comparable arid, high altitude watersheds outside of the immediate study area.

2. Study area

2.1. Physiography and climate

The physiography of the Northern Atacama Region is comprised of several features, including the coastal range (or *Cordillera de la Costa*) separated from the Precordillera by the Central Depression. Pre-Andean basins separate the Precordillera from the Andes (Valero-Garcés et al., 2003). The specific study area encompasses basins of the Andes Mountains, which include Pedernales, Maricunga, and Laguna Verde, as well as the El Salado Bajo, Chañaral, and El Salado Alto basins (Fig. 1a). The highest volcano in the world, the Nevado Ojos del Salado (6893 m s.n.m.; Stern, 2004), closes the Laguna Verde basin to the south (Risacher et al., 1999; Fig. 1a) and marks the southern limit of the central volcanic zone (CVZ) (Stern, 2004).

The Köppen climate classification (Rioseco and Tesser, 2016) indicates that this area within the Atacama Desert is composed of, from west to east: a coastal desert (BWn), normal desert (BWk), cold desert (BWk'), and a dry, steppe-like Andean climate (ETH (ws); Fig. 1b). Additionally, the Andean study area is classified as the *Desert Andes* (north of 31°S), within the *Dry Andes* (north of 35°S). Here, due to limited precipitation and high elevation, only permanent snow patches and small glaciers are found (Lliboutry, 1988 and references therein).

In the Northern Atacama Region, precipitation is scarce. Since 1984, the average precipitation rate in the El Salado River (Las Vegas Station; 26°40′41″ S, 69°39′56″ E) has been 31 mm year^{-1}, with a maximum of 174 mm and 115 mm in 1987 and 2015 respectively. Furthermore, in 2003 and 2007, there was no record of precipitation (MOP, 2017).

2.2. Hydrology

The Northern Atacama Region has four main hydrologic basins, two of which contain hot springs. From west to east these correspond to the El Salado Basin (which is divided into the smaller El Salado Bajo, Chañaral, and El Salado Alto basins) and the naturally endorheic Pedernales, Maricunga, and Laguna Verde basins located within the Puna (Fig. 1a).

The El Salado River originates west of the Andes and its natural headwaters are located downgradient of the Pedernales Basin in a different basin; both are separated by a distance of approximately 200 m (Fig. 1a). The El Salado River drains naturally into the Pacific Ocean at Chañaral. However, in the mid-1970s, it was channeled 10 km to the north of Chañaral, at Caleta Palito (Ramírez et al., 2005; Fig. 1a).

The Pedernales Basin and salt flat, located at 3370 m a.s.l., are the largest of the Atacama Region. There are two hot springs located in this basin: (i) Juncalito, at 4180 m a.s.l., with temperatures ranging between 30 and 40 °C (Hauser, 1997a) and (ii) Río Negro, at 4150 m a.s.l., with an average temperature of 35 °C (Hauser, 1997a; Fig. 1a). The Maricunga Basin and salt flat are located at 3760 m a.s.l. and, after Pedernales, this basin is the second largest in the Northern Atacama Region (Fig. 1a). The Laguna Verde Basin, located within the Puna near the Argentina border at 4350 m a.s.l. (Fig. 1a), is a salty lagoon fed by rivers located generally to the south and west of the basin (Risacher et al., 1999, 2003). The Laguna Verde hot spring, located in the Laguna Verde Basin, is characterized by an average temperature of 40.5 °C (Risacher et al., 1999).

2.3. March 2015 storm event

Despite the aridity of the Northern Atacama Region, intense rain events typically occur once every few years. However, the frequency of storms with the potential to cause flooding in some areas of the Atacama Desert is within the interdecadal (Vargas et al., 2000) to 50 year (Hauser, 1997b) range. Between March 24th and 26th, 2015, the Atacama Region experienced an intense precipitation event resulting from unusual oceanic and atmospheric conditions that produced an inward bound low-pressure cut-off system. Reported rainfall, in the affected areas, ranged between 10 mm on the coast to > 85 mm in the Andes Mountains. Snowfall was also observed over a broad area above 3600 m a.s.l. (Jordan et al., 2015; Fig. 1c).

At the Las Vegas hydro-meteorological station located in the El Salado Alto Basin, reported precipitation within the three-day period was on the order of 80 mm (MOP, 2017). Concentrated, warm, and intense storms resulted in the flooding of the El Salado River (Wilcox et al., 2016). Wilcox et al. (2016) suggested that the March 2015 event was the heaviest and most extensive documented rainfall event within the Northern Atacama Region, producing the largest documented floods compared to adjacent regions. The floods were particularly unusual due

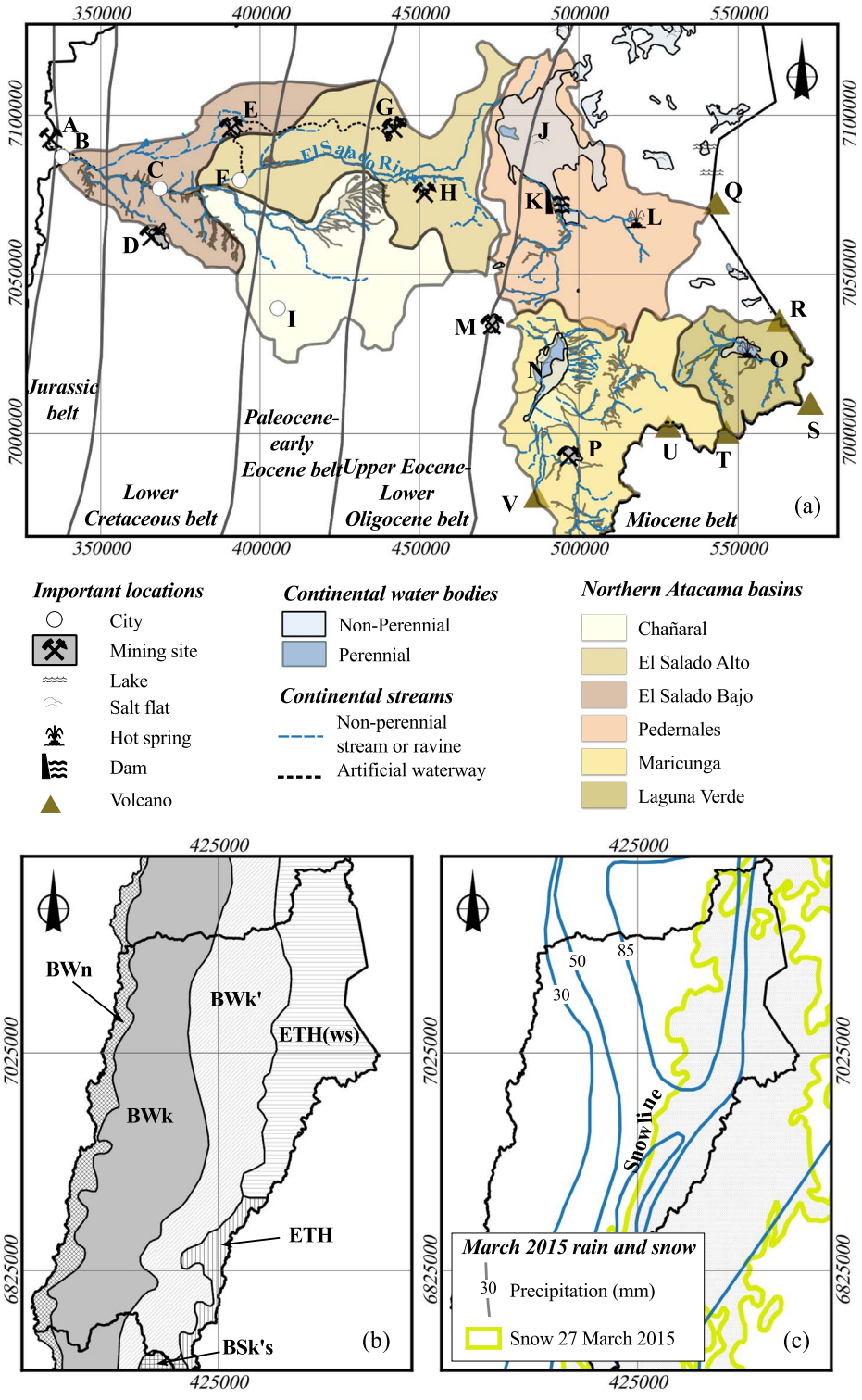

Fig. 1. The Northern Atacama Region. (a) Metallogenic belts (from Sillitoe, 2012; Sillitoe and Perelló, 2005) and basins (from Contreras et al., 2015). The uppercase labels indicate: A. Caleta Palito; B. Chañaral; C. El Salado; D. Manto Verde; E. Pampa Austral Tailings Dam; F. Diego de Almagro; G. El Salvador; H. Potrerillos; I. Inca de Oro; J. Pedernales; K. La Ola Dam; L. Río Negro hot spring; M. La Coipa Mine; N. Maricunga; O. Laguna Verde lake and hot spring; P. Marte Mine; Q: Sierra Nevada de Lagunas Bravas; R: Falso azufre; S: Nevado de Incahuasi; T: Nevado Ojos del Salado; U: El Solo; V: Copiapó Volcano. (b) Climatic zones of the Atacama Region: BWn - coastal desert, BWk - normal desert, BWk' - cold desert, ETH(ws) - cold steppe-like and dry climate of the Andes, ETH - cold steppe-like, and BSk's - cold, semi-arid with winter rain. (c) Precipitation and snow cover during March 27th 2015 (from Jordan et al., 2015).

to their magnitude and high sediment supply, producing highly concentrated sediment flows and extensive mud deposition in urban areas, especially at Diego de Almagro and Chañaral (Fig. 1a). As a result, the aftermath comprised 31 deaths, 16 disappearances, and 30,000 displaced people (Wilcox et al., 2016 and references therein).

2.4. Regional geology and ore deposits

Basement geology, in the distinct physiographic units, is composed of Mesozoic igneous and sedimentary rocks in the *Cordillera de la Costa* as well as Mesozoic to Eocene intrusive and volcanic rocks in the Precordillera; Oligocene to Pliocene basin fill sediments occupy the Central Depression (Clarke, 2006; Fig. 2). At least since 60 Ma, regional geology has been controlled by the CVZ, which is related to subduction of the Nazca plate below the South American plate at a current rate of 7–9 cm year^{-1} (Stern, 2004). In this zone, the continental crust is ≥ 70 km thick and basement ages range from Late Pre-Cambrian to Paleozoic (Stern, 2004; Fig. 2). Cenozoic volcanism in the Atacama Region is related to a number of recent geologic events: (i) Early Miocene to Pleistocene andesite-dacite main arc stratovolcanoes, (ii) early

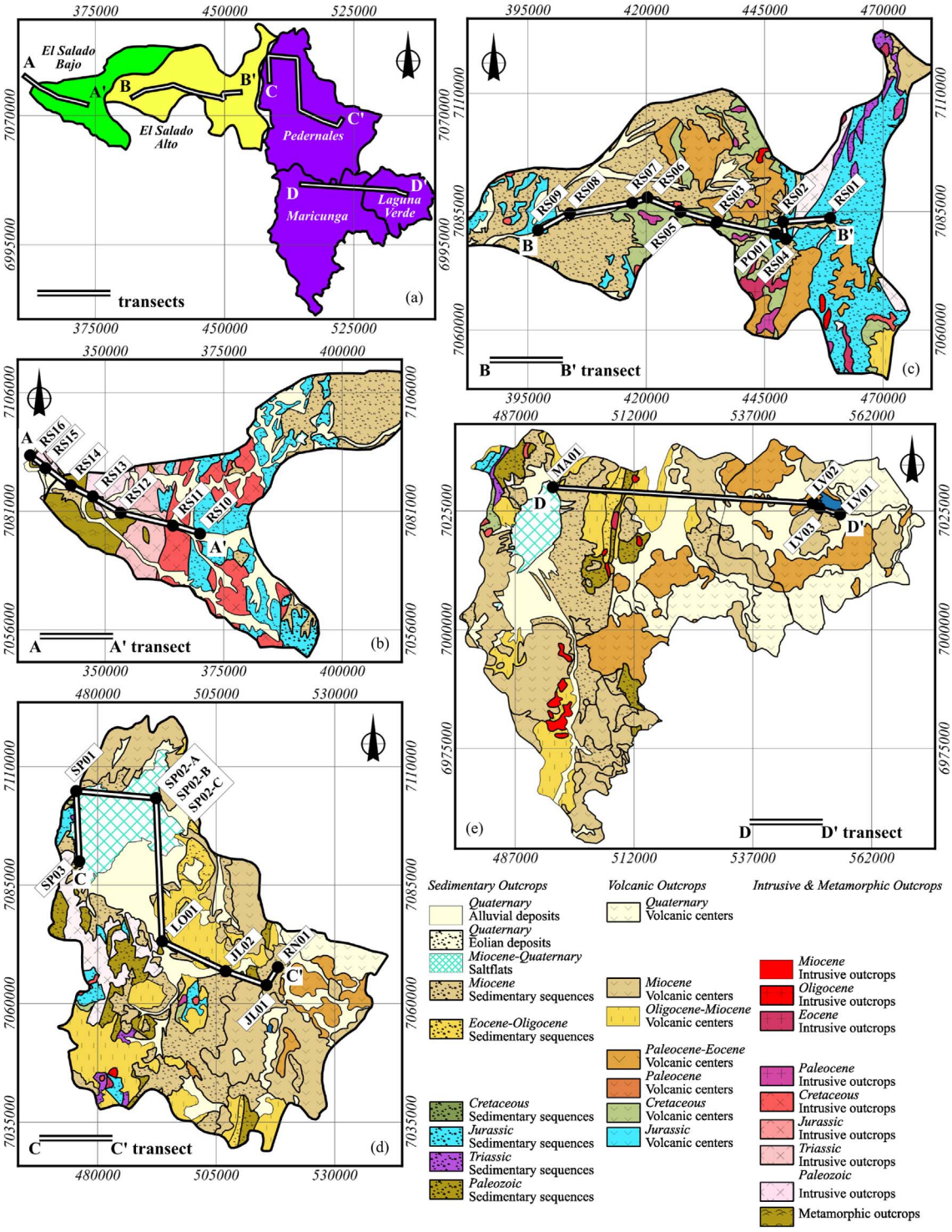

Fig. 2. Geologic maps, sampling sites, and transects. (a) General location map with the basins; (b) El Salado Bajo Basin; (c) El Salado Alto Basin; (d) Pedernales Basin; (e) Maricunga and Laguna Verde basins.

Miocene to Pliocene silicic ignimbrite deposits, and (iii) the formation of lava domes present in both main arc and back-arc regions as well as small Pliocene to Pleistocene basaltic centers in the back arc (Schnurr et al., 2007; Fig. 2).

Ore deposits in the Northern Atacama Region have been classified as longitudinal N-S trending metallogenic belts (Fig. 1a) which, from west to east, correspond to: (i) IOCG and IOA deposits, (ii) Cu-Mo porphyries, and (iii) Au-epithermal and porphyry deposits. Numerous Mesozoic IOCG and IOA ore deposits are hosted in the *Cordillera de la Costa* of northern Chile and are specifically contained within the Upper Jurassic-Lower Cretaceous metallogenic sub-province of the Central Andes (Sillitoe, 2003; Fig. 1a). These deposits include magnetite-dominated, sulfide-poor deposits of the Chilean Iron Belt (Cerro Negro-La Florida; Espinoza, 1990) and productive iron oxide Cu-Au deposits (e.g., Candelaria-Punta del Cobre and Mantoverde districts; Benavides et al., 2007; Fig. 1a). Continuing to the east, Paleocene-Early Oligocene (Sillitoe and Perelló, 2005) and Eocene-Oligocene metallogenic belts are present; in the region, the former holds the Relincho porphyry

copper deposit and the latter holds the Potrerillos (40–32 Ma) and the El Salvador (42–41 Ma) porphyry Cu-Mo deposits. The El Salvador (Fig. 1a) forms part of the major Cu-Mo porphyries in Chile (Cornejo et al., 1997). Farther east, the Miocene metallogenic belt, known as the Maricunga belt, is located in the Andes between 26 and 28°S. Mineralization includes porphyry-type Au and Au-Cu, epithermal Au and Ag-Au high sulfidation, and acid–sulfate-type deposits (Sillitoe et al., 1991). In addition, salt flats located in the Altiplano-Puna plateau, such as the Maricunga and Pedernales, have an estimated Li reserve of 280,000 and 240,000 tons respectively (Gajardo, 2014). The Maricunga salt flat is composed of a halite and gypsum crust where an ulexite ($NaCaB_5O_9{\cdot}8H_2O$) deposit is hosted (Risacher et al., 1999).

2.5. Anthropogenic activities and historical contamination of the El Salado River

The primary anthropogenic activities in the study area include the exploration, exploitation, and smelting of ores. The exploitation of seams and veins in the Potrerillos district, from 1894 to 1940, began the first of a series of anthropogenic developments in the region (Biblioteca Nacional de Chile, 2017; Olson, 1989). Activity continued in 1959 with the exploitation of the El Salvador porphyry copper deposit, producing an average of 81 thousand metric tons of copper per year between 1960 and 2015 (SONAMI, 2017).

In the 1930s, a tunnel was drilled to divert salty water from the Pedernales into the El Salado River (Risacher et al., 1999), transforming a naturally non-endorheic Pedernales Basin into an artificially exorheic basin (Risacher et al., 1999; Fig. 3a). Between 1938 and 1975, mining activities linked to Potrerillos and El Salvador resulted in the disposal of nearly $150{\cdot}10^6$ tons of tailings without treatment into the El Salado River flowing directly into Chañaral Bay, creating approximately 3.6 km^2 of artificial beach. This artificial feature extends nearly 5 km N-S and is 0.40 to 0.88 km wide (*E*–W) with an approximate thickness of 9 m at the center (Castilla, 1983 and references therein). In 1976, the El Salado was routed, via an artificial waterway, to Caleta Palito, a rocky beach located approximately 10 km north of Chañaral (Fig. 3b) and 10 km south of the Pan de Azúcar National Park. Between 1976 and 1990, $126{\cdot}10^6$ to $150{\cdot}10^6$ tons of solid waste were discharged forming a second artificial beach at Caleta Palito. Analyses of mine tailing waste water exhibited total Cu concentrations between 6 and 7 mg L^{-1} (Castilla, 1983 and references therein). In March 1990, the Supreme Court of Chile ruled that discharging waste from the El Salvador Mine into the El Salado River was to be prohibited. Consequently, the mining company was required to build a tailings dam at Pampa Austral (Fig. 1a). Currently, this dam is only permitted to discharge "clean water" into the El Salado River that contains < 2 mg L^{-1} total Cu (Castilla, 1996).

Presently, the Potrerillos facilities function as a copper smelter (Fig. 3c) and the largest mining operations are being developed simultaneously at sites in the *Cordillera de la Costa* and in the Andes. For example, in the *Cordillera de la Costa*, Mantos Copper (formerly Anglo American Norte) has produced, on average, 124 thousand metric tons of copper per year between 1990 and 2015 (SONAMI, 2017). Recent exploration activities in the Andes have permitted the discovery of Caspiche and Cerro Maricunga (COCHILCO, 2016) as well as the estimation of Li reserves in salt flats (Gajardo, 2014).

3. Analytical methods

3.1. Sampling

Superficial water and fluvial sediments were sampled within the El Salado basins (RS01 to RS16 and PO01; Fig. 2a,b,c), the Pedernales Basin (Fig. 2a,d), and the Maricunga and Laguna Verde basins (Fig. 2a,e). For more details, Fig. 2 is further separated into the respective basins sampled (b–e).

The El Salado River was sampled approximately every 5 km along its course in an *E*–W trending, downstream direction. The Pedernales

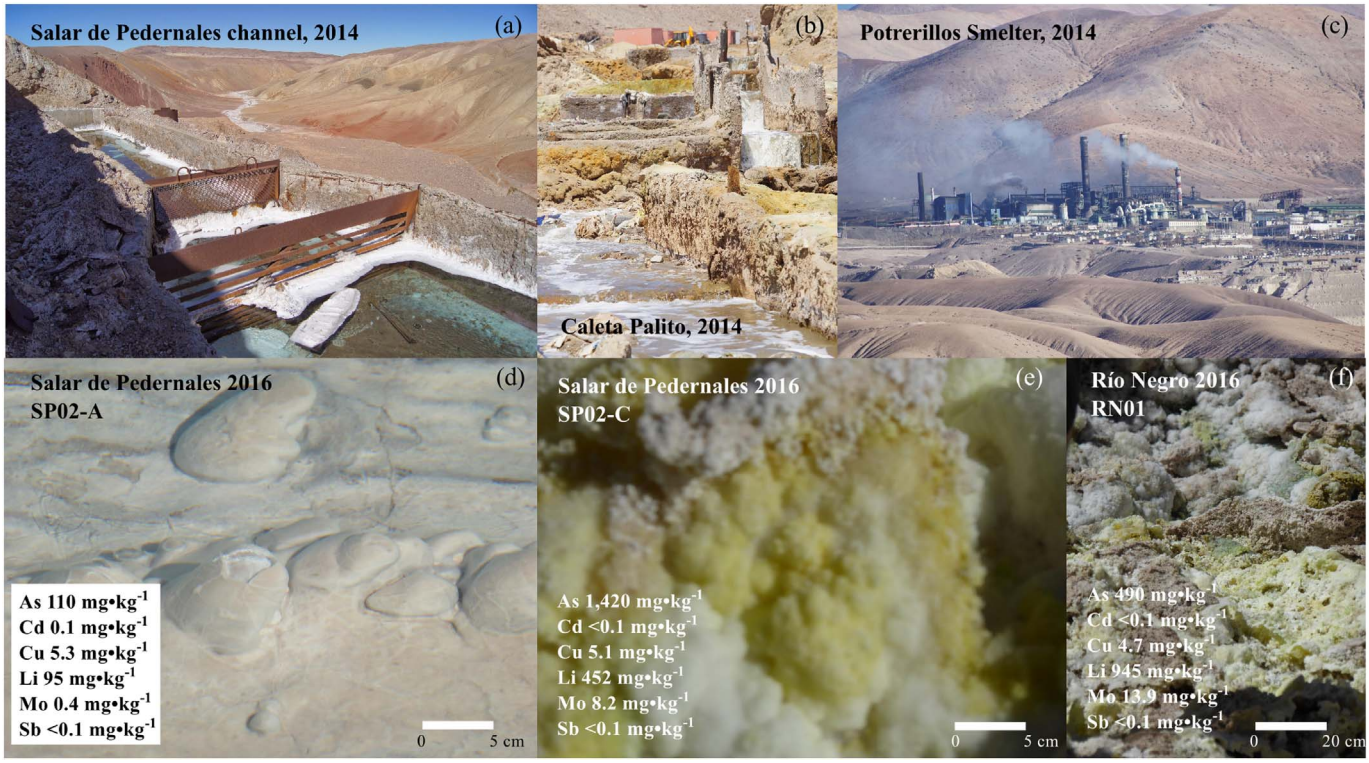

Fig. 3. Important locations and chemical deposits in the Northern Atacama Region. (a) Channel of the Pedernales salt flat in 2014; (b) Caleta Palito in 2014; (c) Potrerillos Smelter in 2014. (d) Chemical precipitate in the Pedernales salt flat, found in 2014 and 2016 and sampled in 2016; (e) Chemical precipitate in the Pedernales salt flat, found in 2016; (f) Chemical precipitate in the Río Negro hot spring, found in 2016.

Basin was sampled in the man-made outlet (SP01; Fig. 3a), the eastern lake of the Pedernales salt flat (SP02), the southwest border of the Pedernales salt flat (SP03), the La Ola Dam (LO01), the Juncal River (JL01 and JL02), and the Río Negro hot spring (RN01). Maricunga was sampled in the northern limit (MA01) and Laguna Verde was sampled along the eastern and western borders (LV01 and LV02) as well as in the hot spring (LV03).

At each site, pH was measured using a field pH-meter. All water samples were taken in the upper 5 cm of the river using a previously homogenized syringe. 100 mL were filtered through an acetate syringe filter (0.22 μm) into a previously acid-cleaned polypropylene vial. Previous tests made with water samples of this area showed that there was no significant difference in the concentration of the studied elements using 0.22 or 0.45 μm filters. In addition, work conducted by Leybourne and Cameron (2008) in the Spence Deposit, north of the sampling sites, indicated that there is no difference in the concentrations of filtered versus unfiltered trace elements in the area. Therefore the metal and metalloid species identified in this study are the dissolved (0.22 μm filter) and particulate (< 63 μm) fractions. Samples were acidified in the field (pH ~2 with suprapure HNO_3) and were stored at 4 °C until analysis.

At sites with available sediments, approximately 500 g were retrieved from the top 5 cm of 1 m^2 representative areas using acid-cleaned plastic instruments. In addition, in 2016 two precipitates were collected at Pedernales (SP01-A and SP02-C; Figs. 3d,e) and one was collected at Río Negro (RN01; Fig. 3f). Despite the fact that sediments from Potrerillos site (PO01) were sampled during all field campaigns (2014–2016), samples from 2014 and 2015 were misplaced and therefore not analyzed. After collection, these samples were stored in sealed sampling bags at 4 °C until analysis. The sampled sediments were dried in the laboratory at 50 °C. Afterwards, 2014 sediments were homogenized with an agate mortar, and 2015–2016 sediments were sieved (63 μm) for geochemical quantification.

The easternmost basins, i.e. Pedernales, Laguna Verde, and Maricunga, were not sampled during 2015 due to difficulties accessing these sites after the flooding of the El Salado River.

3.2. Water and sediment analyses

Geochemical analyses of water samples collected in 2014 were performed using a quadrupole ICP-MS at the GET Laboratory (Toulouse, France) and elemental concentrations were certified by the SLRS-5 water standard. Water samples collected during the 2015 and 2016 field campaigns were analyzed at the Helmholtz Centre for Environmental Research in Magdeburg, Germany.

For trace elements, river sediments were digested with an aqua regia solution according to the norm ISO 15587-1 (2002). Measurements of the diluted (2015 and 2016) and digested solutions were determined using an ICP-MS (Varian 8800) following the methods described in EN ISO 17294-2 (2016).

Independently measured sediment standards were incorporated in the daily procedure during each analysis for quality assurance. Independent from the certified reference material LGC6187 Batch 01, sample 0192 (river sediment – extractable metals) was used to verify that recovery rates for the analyzed elements were within the given certified range. The performed ongoing annual method validation established a minimum level of quantification in addition to the maintenance of calibration curve linearity and homoscedasticity of variance within the working range. Successful participation in a yearly inter-laboratory test, organized by r-concept, assured quality data production with the analytical methods used in this study. Element concentrations of all sediments and precipitates were quantified at the Helmholtz Centre for Environmental Research in Magdeburg, Germany.

3.3. Element selection, local geochemical background, and environmental indices

Before data treatment, all values below the detection limit (DL) were recalculated as the DL divided by 2. Samples SP02A-2016 (Fig. 3c), SP02C-2016 (Fig. 3d), and RN01-2016 (Fig. 3e) were not included in the statistical analysis of fluvial sediments as they correspond to chemical precipitates. Subsequently, the comparison of analyzed elements in the sampled fluvial water with average global concentrations of worldwide rivers (Gaillardet et al., 2003) demonstrated that As, Li, Mo, and to a lesser extent Cd, Cu and Sb are elevated. A comparison between the analyzed elements in the sediments and elemental concentrations in the upper continental crust (UCC; Rudnick and Gao, 2003) demonstrates that As, Cu, Li, Mo, and Sb are elevated with respect to the UCC. Therefore, As, Cd, Cu, Li, Mo, and Sb were selected in an effort to accomplish the objectives presented in the introduction.

Previous research from State Chilean Agencies has concluded that the concentration of certain elements in northern Chile in the dissolved form, namely As, tends to remain constant (DGA, 2014). Therefore, the goal of this study was to calculate the normal concentration of the selected elements in fluvial water and sediments of the Northern Atacama Region, including the geogenic and anthropogenic signatures, which here is referred to as the *local geochemical background*. To calculate the local geochemical background within this region for the dissolved and particulate form, two previously used methodologies were employed: percentiles (Tapia et al., 2012) and the iterative 2σ technique (Gałuszka et al., 2015; Matschullat et al., 2000). For the percentile method, values within the 0.25–0.75 percentile were considered the local geochemical background. For the iterative 2σ technique, the average and standard deviation (σ) were obtained. Afterwards all values beyond the ± 2σ level were discarded and a new average and σ were obtained; subsequently, a ± 2σ range using the reduced data was calculated. This procedure was repeated until all values lied within this range, i.e. until they approached a normal distribution (Gałuszka et al., 2015).

To infer water quality, recommendations of the World Health Organization (WHO, 2011), the United States Environmental Protection Agency (US EPA, 2009), and Chilean Guidelines (NCH 409, 2006) were employed. In the case of Li, despite the absence of a guideline, Aral and Vecchio-Sadus (2008) indicate that concentrations > 20 mg L^{-1} might entail a risk of death. To infer sediments quality, current Chilean regulations have not established guidelines for element concentrations. Due to the lack of these values, sediment concentrations were compared to the interim sediment quality guideline (ISQG) and probable effect level (PEL) of the Canadian legislation (Canadian Council of Ministers of the Environment, 2001), where there are guidelines for As, Cu and Cd. Sediment quality for Li, Mo and Sb were not studied.

To infer the degree of contamination and probable sources of As, Cd, Cu, Li, Mo, and Sb in sediments, geo-accumulation indices (Eq. 1, I_{geo}; Muller, 1979) and enrichment factors (Eq. 2, EFs; Zoller et al., 1974) were calculated using the following local background values: the average concentration of Atacama regolith from 30 cm depth (López, 2014), rocks from the La Negra (andesites to basaltic andesites; López, 2014; Oliveros et al., 2007) and Punta del Cobre (López, 2014) Formations, the Llano San Pedro volcanic sequence (López, 2014), ignimbrites (López, 2014), and the chemical precipitates obtained from the field campaign (Fig. 3d to f). All these materials (regolith, rocks and precipitates) belong to the Northern Atacama Region, rocks and regolith are specifically located in the Chañaral Basin (Fig. 1a), within a 100 km radius of the study area.

$$I_{geo} = \log_2\left(\frac{C_n}{1.5 \times B_n}\right) \quad (1)$$

In Eq. 1, C_n corresponds to the measured concentration of metal *n* in the sediment, and B_n is the local background value for the metal *n*. The

factor 1.5 is used for possible variations of the local background due to variable lithologies (Muller, 1979; Nowrouzi and Pourkhabbaz, 2014). For each sediment sample, the I_{geo} index indicates the following:

i. $I_{geo} \leq 0$, the sample is not contaminated.
ii. $0 < I_{geo} \leq 1$, the sample is non-to-slightly contaminated.
iii. $1 < I_{geo} \leq 2$, the sample is moderately contaminated.
iv. $2 < I_{geo} \leq 3$, the sample is moderately to highly contaminated.
v. $3 < I_{geo} \leq 4$, the sample is highly contaminated.
vi. $4 < I_{geo} \leq 5$, the sample is highly to extremely contaminated.
vii. $I_{geo} > 5$, the sample is extremely contaminated.

$$EF = \frac{M_{sample}/Fe_{sample}}{M_{background}/Fe_{background}} \quad (2)$$

In Eq. 2, M_{sample}/Fe_{sample} corresponds to the ratio of the concentration of the metal (of interest) to iron in the sample and $M_{background}/Fe_{background}$ is the ratio of the local background concentration of the metal to the local background concentration of iron (Zoller et al., 1974).

To infer possible sources, calculated EF values near 1 indicate that the trace metal originates from crustal contributions, is not enriched (Chen et al., 2007; Zhang and Liu, 2002), and could originate from the same rock, regolith, or precipitate with which it was calculated (Zoller et al., 1974). High values signify that the sample does not originate from that Earth material. Regarding EFs, Fe was used as the normalizing element because local background concentrations are readily provided in the literature for rocks of the Atacama Region (López, 2014; Oliveros et al., 2007).

4. Results

Results are presented for the various sampling areas as a function of surface elevation and are grouped as follows: the Andes Mountain basins (i.e. the Pedernales, Maricunga and Laguna Verde basins), the El Salado Alto Basin, and the El Salado Bajo Basin. Surface elevations are the highest in the Andes Mountains and they decrease toward the coast. The average site elevation within the studied basins of the Andes Mountains is 3832 m a.s.l. In contrast, the average surface elevations in the El Salado Alto and El Salado Bajo basins are 1583 and 191 m a.s.l., respectively.

4.1. Andes Mountains basins

4.1.1. Area-specific geology

The Andes Mountains contain the Pedernales (Fig. 2d), Maricunga and Laguna Verde (Fig. 2e) basins. This environment is mostly constituted by Eocene to Miocene continental, marine, and volcanic sedimentary sequences as well as Paleocene to Quaternary volcanic complexes, volcanic centers, and ignimbrites. Paleozoic to Cretaceous outcrops are very scarce in this area when compared to the El Salado Alto and Bajo basins, respectively, and Cenozoic outcrops are predominant (Fig. 2). The Pedernales Basin contains a mixture of sediments originating from volcanic and intrusive rocks (Risacher et al., 1999). The Maricunga Basin includes a mixture of volcanic formations, plutonic rocks, and sediments (Risacher et al., 1999).

4.1.2. Enriched elements in water and sediments

In these basins, the most enriched elements in superficial water when compared to the average concentration of worldwide rivers (from Gaillardet et al., 2003; Table 1) correspond to Li (44,135 times global average) > As (9444 times global average) > Mo (861 times global average) and to a lesser extent Sb, Cd and Cu (24, 21 and 2 times global average, respectively).

In fluvial sediments, the most enriched elements when compared to the upper continental crust (from Rudnick and Gao, 2003; Table 2) correspond to As (35 times global average) > Mo (33 times global average) > Cd (14 times global average) and to a lesser extent Li and Cu (7 and 6 times the global average respectively); Sb is not enriched.

4.1.3. Elements and regulations

In the Andes Mountains, 100% of the samples present surficial water values above the recommendations of the WHO, US EPA, and Chilean Guidelines for As; 73% of the values are above the WHO recommendation for Mo and 40% of the samples exhibit concentrations over the literature recommendation for Li (Fig. 4). On the contrary, only 13% of the samples have higher values than the WHO and EPA recommendations and no samples are above the NCH 409 for Cd. Only 6% of the samples are above the WHO and US EPA recommendations for Sb and all values of Cu are well below national and international recommendations for water (Fig. 4).

In the case of sediments, all As values are above the ISQG, while 88% of the samples are above the PEL; for Cd, 47% of the samples are above the ISQG and 6% above the PEL, and for Cu, 47% of the values are above the ISQG and 29% are above the PEL (Fig. 5).

4.1.4. Local geochemical background for water and sediments, contaminant elements, and probable sources

In the Andes, using the 0.75 percentile (Tapia et al., 2012) and iterative 2σ techniques (Gałuszka et al., 2015; Matschullat et al., 2000), in surface water the highest local geochemical background was observed for As, and depending on the statistical method used, Li and Mo (Table 3a). In sediments, the maximum values of local geochemical background using the 0.75 percentile and iterative 2σ methods are found in the Andes Mountains basins for As, Cd, and Li (Table 3b).

In relation to probable contaminant elements in the Andes Mountains basins, I_{geo} index indicate that Cu corresponds to a contaminant of this environment, especially during 2016 (Fig. 6); As, Cd, Li, and Sb are not considered contaminants in this area. Regarding Mo, in 2014 it was not considered a contaminant; however, in 2016 it became one. In general, the level of contamination tended to increase from 2014 to 2016 (Fig. 6).

In relation to the sources of the studied elements, except for Cu, EFs indicate that these elements might have originated from local precipitates obtained from remote areas of the Andes; the Atacama regolith might also be a source of Cd and Sb. Other Atacama rocks from the Chañaral Basin do not indicate that they could be the source of these elements (Fig. 7).

4.2. El Salado Alto basin

4.2.1. Area-specific geology

Geology at the location of El Salado Alto Basin is constituted by Jurassic marine and continental sedimentary sequences, Jurassic, Cretaceous and Paleocene-Eocene volcanic centers, domes and ignimbrites, and Miocene marine and continental sedimentary sequences. Mesozoic and Cenozoic rocks are predominant (Fig. 2c).

4.2.2. Enriched elements in water and sediments

In this basin, the most enriched elements in surficial water when compared to worldwide rivers (from Gaillardet et al., 2003; Table 1) are Li (78,662 times global average) > As (2787 times global average) > Mo (680 times global average) > Sb (72 times global average) and to a lesser extent Cd and Cu (17 and 14 times global average, respectively).

Sediments compared to the average respective concentrations of the UCC (from Rudnick and Gao, 2003; Table 2) indicate that in the El Salado Alto Basin they are enriched as follows (in decreasing order): Cu (50 times global average) > As (23 times global average) > Mo (19 times global average) and to a lesser extent Sb, Li, and Cd (7, 4.5, and 3.6 times the global averages, respectively). The Potrerillos sample collected in 2016 shows the highest concentrations of As, Cd, Cu, Mo,

Table 1
Basic statistics for water concentration values in all samples collected in the Andes Mountains and El Salado Alto and El Salado Bajo basins for As, Cd, Cu, Li, Mo and Sb. Also shown: the average concentration for these elements worldwide (Gaillardet et al., 2003) and the concentration for drinkable water recommended by the World Health Organization (WHO, 2011), the US Environmental Protection Agency (US EPA, 2009), Chilean regulations (NCH 409, 2006), and Aral and Vecchio-Sadus (2008).

	All samples of Northern Atacama Region						Andes mountains						El Salado Alto						El Salado Bajo					
	As	Cd	Cu	Li	Mo	Sb	As	Cd	Cu	Li	Mo	Sb	As	Cd	Cu	Li	Mo	Sb	As	Cd	Cu	Li	Mo	Sb
	$\mu g\cdot L^{-1}$	$\mu g\cdot L^{-1}$	$\mu g\cdot L^{-1}$	$mg\cdot L^{-1}$	$\mu g\cdot L^{-1}$	$\mu g\cdot L^{-1}$	$\mu g\cdot L^{-1}$	$\mu g\cdot L^{-1}$	$\mu g\cdot L^{-1}$	$mg\cdot L^{-1}$	$\mu g\cdot L^{-1}$	$\mu g\cdot L^{-1}$	$\mu g\cdot L^{-1}$	$\mu g\cdot L^{-1}$	$\mu g\cdot L^{-1}$	$mg\cdot L^{-1}$	$\mu g\cdot L^{-1}$	$\mu g\cdot L^{-1}$	$\mu g\cdot L^{-1}$	$\mu g\cdot L^{-1}$	$\mu g\cdot L^{-1}$	$mg\cdot L^{-1}$	$\mu g\cdot L^{-1}$	$\mu g\cdot L^{-1}$
N	65	65	65	22	65	65	16	16	16	5	16	16	28	28	28	10	28	28	21	21	21	7	21	21
Average	2039	1.24	9.62	87	248	2.79	5502	1.48	0.93	81	397	2.00	1513	1.31	12.64	145	283	4.67	103	0.96	12.22	10	86	0.88
Standard deviation (σ)	4461	1.36	14.55	92	335	9.27	8001	2.47	1.15	110	594	6.05	1126	0.83	18.60	78	180	13.24	158	0.55	11.39	1.7	56	1.32
Median	618	1.04	2.35	12	161	0.35	900	0.59	0.25	2.9	230	0.43	1040	1.42	2.01	163	229	0.51	19	1.06	6.58	9	92	0.25
Maximum	24,751	8.49	60.97	228	2404	65	24,751	8.49	3.98	225	2404	24.65	4035	3.11	60.97	228	571	64.75	495	1.76	42.18	13	214	5.65
Minimum	2	0.10	0.25	1.5	0.25	0.07	79	0.10	0.25	1.5	0.25	0.25	75	0.10	0.25	5.1	10	0.20	2	0.15	0.25	8.6	18	0.07
Correlation coefficient element-elevation	0.41	0.09	−0.30	0.16	0.34	0.12	−0.24	−0.44	−0.25	−0.95	0.13	0.18	0.13	0.08	−0.02	−0.20	−0.12	0.29	−0.13	−0.07	−0.59	0.94	−0.06	0.03
World average	0.62	0.08	1.48	0.002	0.42	0.07																		
WHO recommendations	10	3	2000	–	70	20																		
US EPA guideline	10	5	1300	–	–	6																		
Chilean regulation	10	10	2000	–	–	–																		
Aral and Vecchio-Sadus (2008)	–	–	–	20	–	–																		

Table 2
Basic statistics for fluvial sediment compositions, namely of As, Cd, Cu, Li, Mo and Sb in all samples collected in the Andes Mountains, the El Salado Alto Basin, and the El Salado Bajo Basin. The average composition of the UCC (Rudnick and Gao, 2003), the Canadian interim sediment quality guideline of Canada (ISQG), and the Canadian probable effects level (PEL; Canadian Council of Ministers of the Environment, 2001).

	All samples of Northern Atacama Region						Andes mountains						El Salado Alto						El Salado Bajo					
	As	Cd	Cu	Li	Mo	Sb	As	Cd	Cu	Li	Mo	Sb	As	Cd	Cu	Li	Mo	Sb	As	Cd	Cu	Li	Mo	Sb
	$\mu g{\cdot}g^{-1}$	$\mu g{\cdot}g^{-1}$	$\mu g{\cdot}g^{-1}$	$\mu g{\cdot}g^{-1}$	$\mu g{\cdot}g^{-1}$	$\mu g{\cdot}g^{-1}$	$\mu g{\cdot}g^{-1}$	$\mu g{\cdot}g^{-1}$	$\mu g{\cdot}g^{-1}$	$\mu g{\cdot}g^{-1}$	$\mu g{\cdot}g^{-1}$	$\mu g{\cdot}g^{-1}$	$\mu g{\cdot}g^{-1}$	$\mu g{\cdot}g^{-1}$	$\mu g{\cdot}g^{-1}$	$\mu g{\cdot}g^{-1}$	$\mu g{\cdot}g^{-1}$	$\mu g{\cdot}g^{-1}$	$\mu g{\cdot}g^{-1}$	$\mu g{\cdot}g^{-1}$	$\mu g{\cdot}g^{-1}$	$\mu g{\cdot}g^{-1}$	$\mu g{\cdot}g^{-1}$	$\mu g{\cdot}g^{-1}$
N	42	42	42	42	42	42	14	14	14	14	14	14	20	20	20	20	20	20	8	8.0	8	8	8	8
Average	121	0.6	932	127	29	2.0	170	1.3	178	155	37	0.2	109	0.3	1387	94	21	3.0	66.1	0.3	1114	163	37	2.8
Standard deviation (σ)	117	1.2	2396	148	67	5.5	151	2.0	207	207	97	0.2	103	0.3	3256	46	46	7.3	24.5	0.0	1734	195	52	4.9
Median	74	0.3	233	78	4.4	0.5	162	0.9	95	69	1.9	0.1	73	0.3	182	90	4.4	0.5	60.2	0.3	393	78.3	8.5	0.8
Maximum	571	7.7	14,600	799	345	33	571	7.7	643	799	345	1	463	1.5	14,600	202	210	33	117.0	0.3	5340	630	155	15
Minimum	8	0.1	7	19	0.2	0.1	8	0.1	7	19	0.2	0.1	18	0.1	17	29	0.9	0.1	38.1	0.2	235	58.3	5.2	0.6
Correlation coefficient element-elevation	0.37	0.27	−0.14	−0.01	−0.002	−0.15	−0.03	−0.58	−0.41	−0.47	−0.49	−0.04	0.41	0.30	0.18	0.08	0.21	0.20	−0.80	−0.33	−0.47	−0.41	−0.48	−0.52
UCC	4.8	0.09	28	21	1.1	0.4																		
ISQG	5.9	0.6	35.7	–	–	–																		
PEL	17	3.5	197	–	–	–																		

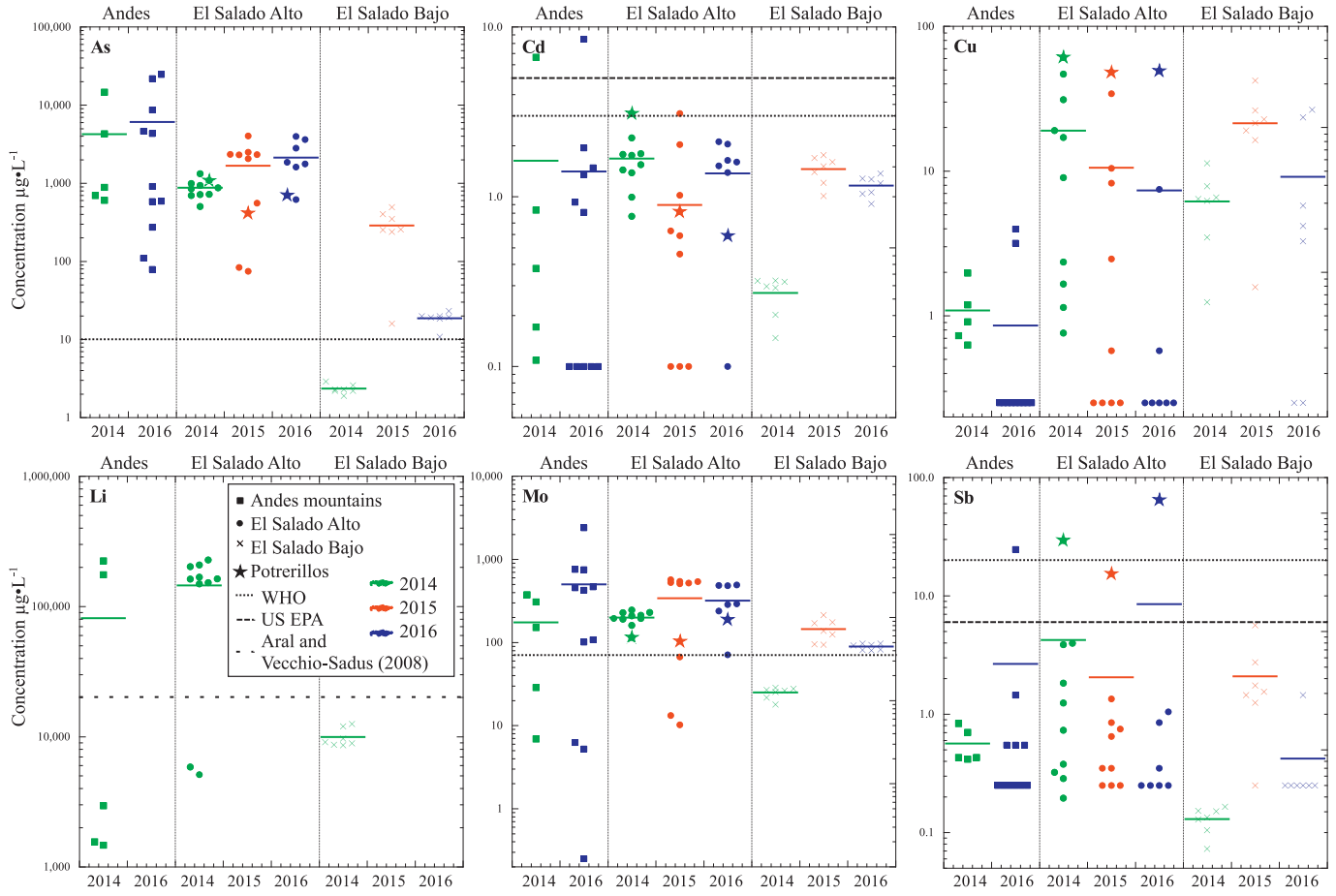

Fig. 4. Element concentrations as a function of the sample year in surface water from the Andes Mountains and El Salado Alto and El Salado Bajo basins. Continuous lines represent the average element concentration of surface water in each area and dashed lines represent concentrations suggested as drinkable by the US EPA (As, Sb; US EPA, 2009), WHO (As, Cd, Mo; WHO, 2011), Chilean regulation (As; NCH 409, 2006), and Aral and Vecchio-Sadus (2008; Li).

and Sb in collected sediments of El Salado Alto Basin (Fig. 8).

4.2.3. Elements and regulations

In El Salado Alto Basin, dissolved As concentrations are above the WHO, US EPA, and NCH 409 in all samples. For Mo, 89% of the samples are above the WHO recommendation and 80% of the samples are above the Aral and Vecchio-Sadus (2008) recommendation for Li (Fig. 4). In the case of Cd, only 7% of the samples are above the WHO recommendation and no samples are above the US EPA and Chilean regulations. For Sb, 7% and 11% are above the WHO and US EPA regulations, respectively, and Cu is below all normatives (Fig. 4).

In sediments, 100% of the samples are above the PEL for As. In the case of Cd, just 5% are above the ISQG and none above the PEL. For Cu, 95% of the samples are above the ISQG and 45% are above the PEL (Fig. 5).

4.2.4. Local geochemical background for water and sediments, contaminant elements, and probable sources

The highest local geochemical background for dissolved Cd is found in El Salado Alto, and depending on the employed statistical method, Li and Mo as well (Table 3a). In sediments, the highest local geochemical background is not present in this basin for any of the studied elements (Table 3b).

Regarding the probable contaminants of El Salado Alto Basin, the I_{geo} index indicates that Cu and Mo might be contaminants (Fig. 6).

In relation to probable sources, local precipitates can explain the presence of As and Li; the Punta del Cobre Formation could explain the concentration of As, and the Atacama regolith might explain the values of Cd and Sb (Fig. 7). None of the local background precipitates, rocks, and regolith used to calculate EFs can explain the elevated I_{geo} index for Cu and Mo. This enhances the idea that these elements correspond to contaminants of the El Salado Alto Basin (Fig. 7).

4.3. El Salado Bajo basin

4.3.1. Area-specific geology

El Salado Bajo Basin is constituted mostly of Jurassic sedimentary and volcanic sequences, Cretaceous, Jurassic and Paleozoic intrusive rocks, and metamorphic Paleozoic outcrops. Younger outcrops are scarce, and are comprised of Miocene sedimentary sequences and Quaternary alluvial and eolian deposits (Fig. 2b).

4.3.2. Enriched elements in water and sediments

In fluvial water, the most enriched elements in comparison to rivers worldwide (from Gaillardet et al., 2003; Table 1) are Li (5398 times global average) > Mo (206 times global average) > As (167 times global average) and to a lesser extent Sb, Cd, and Cu (14, 13, and 9 times global average, respectively).

Sediments compared to the average respective concentrations of the UCC (from Rudnick and Gao, 2003; Table 2) indicate that in the El Salado Bajo, elements are enriched as follows (in decreasing order): Cu (40 times global average) > Mo (33 times global average) > As (14 times global average) and to a lesser extent Li, Sb and Cd (8, 7 and 3 times global average, respectively).

As shown, enrichments of fluvial water and sediments are in general lower in this basin compared to the Andes Mountains and El Salado Alto

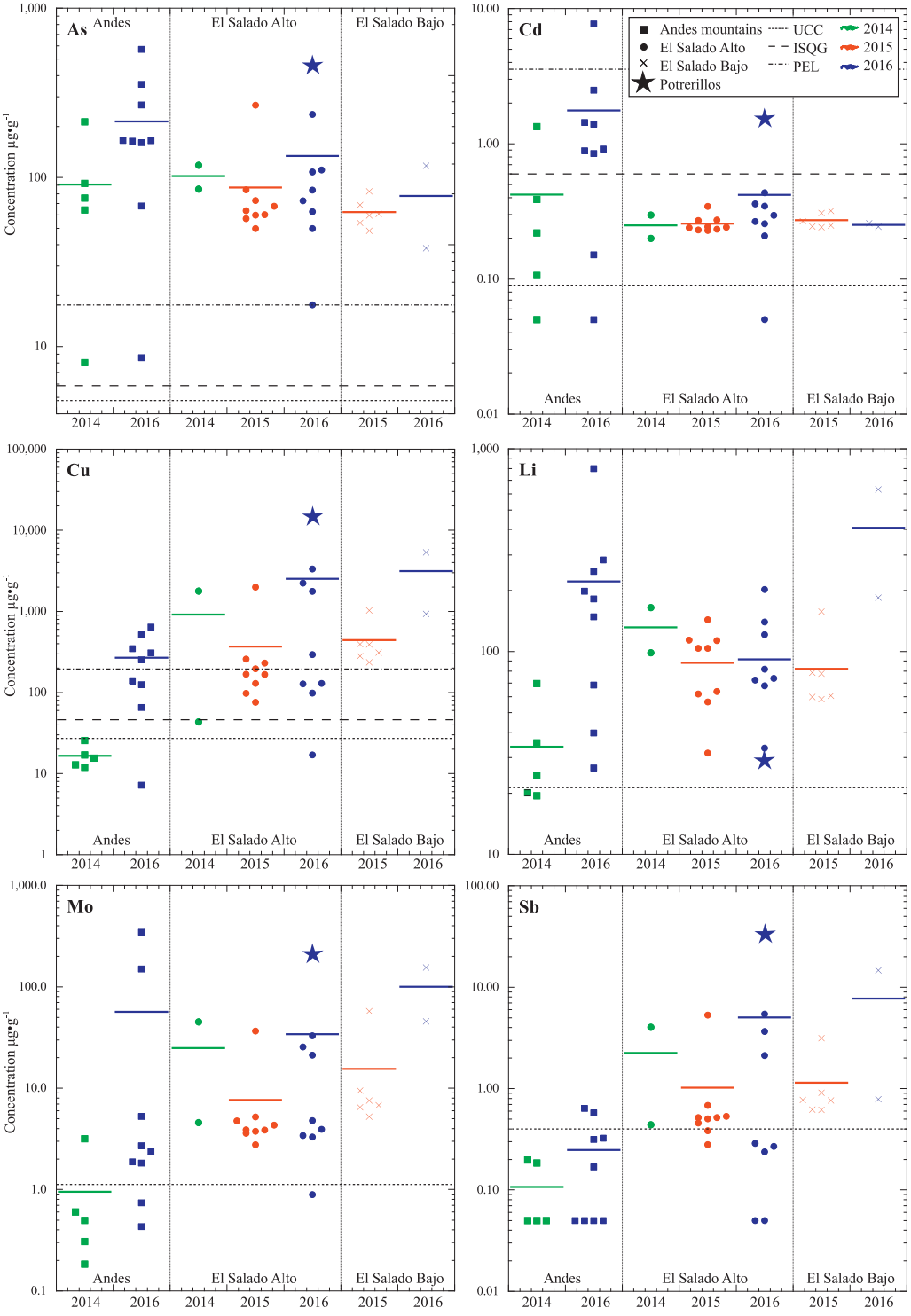

Fig. 5. Element concentrations as a function of the sample year in fluvial sediments of the Andes Mountains and El Salado Alto and El Salado Bajo basins. Continuous lines represent the average concentrations of sediments within each basin. UCC: Upper continental crust (Rudnick and Gao, 2003); ISQG: Canadian interim sediment quality guideline from Canada; PEL: Canadian probable effects level (Canadian Council of Ministers of the Environment, 2001).

basins.

4.3.3. Elements and regulations

For As and Mo, 63% of water samples present concentrations above the WHO, US EPA, or Chilean regulations. All samples with values below recommendations were taken during 2014, before the Atacama storm event and landslide. In addition, all samples values are below the national and international recommendations for Cd, Cu, Li, and Sb (Fig. 4).

In the case of sediments, for As and Cu, all samples show values above the ISQG and PEL. For Cd, all are below the ISQG and PEL (Fig. 5).

4.3.4. Local geochemical background for water and sediments, contaminant elements, and probable sources

The highest local geochemical background for dissolved Cu was obtained in this basin in addition to Sb when using the 0.75 percentile (Table 3a). In sediments, the highest local geochemical background was obtained in El Salado Bajo Basin for Cu, Mo, and Sb (Table 3b).

In relation to probable contaminants, I_{geo} index indicates that Cu, Mo, and Sb might be considered contaminants in this basin in contrast to As, Cd, and Li (Fig. 6).

Table 3
Local geochemical background of mining sites worldwide. (a) Dissolved water in Oruro; (b) Lake sediments in Oruro, fluvial sediments in Chalkidiki and the Northern Atacama Region basins, and soil in the Miedzianka Mountains. P 0.75: percentile 0.75; 2σ: maximum value of iterative 2σ technique (Gałuszka et al., 2015). Oruro (Tapia et al., 2012; Tapia and Audry, 2013; Li and Mo concentrations in pore water and sediments are unpublished data); Miedzianka Mountains (Gałuszka et al., 2015); Chalkidiki (Kelepertzis et al., 2010).

(a)

		Oruro, Bolivia		All samples of Northern Atacama Region		Andes mountains		El Salado Alto		El Salado Bajo	
		P 0.75	2σ	P 0.75	2σ	P 0.75	2σ	P 0.75	2σ	P 0.75	2σ
As	$\mu g \cdot L^{-1}$	740	902	1857	1032	5659	5073	2316	2832	238	28
Cd	$\mu g \cdot L^{-1}$	0.03	0.04	1.60	2.28	1.38	1.53	1.78	2.55	1.37	2.05
Cu	$\mu g \cdot L^{-1}$	0.74	0.86	11.35	0.61	0.98	0.25	18	0.57	21	29
Li	$mg \cdot L^{-1}$	0.04	0.06	167	272	175	301	194	300	11	13
Mo	$\mu g \cdot L^{-1}$	21	31	307	259	459	795	489	643	97	178
Sb	$\mu g \cdot L^{-1}$	10	12	1.24	0.36	0.59	0.71	1.27	0.86	1.45	0.32

(b)

		Oruro, Bolivia		Miedzianka Mt., Poland		Chalkidiki, Greece		All samples of Northern Atacama Region		Andes mountains		El Salado Alto		El Salado Bajo	
		P 0.75	2σ	P 0.75	2σ	P 0.75	2σ	P 0.75	2σ	P 0.75	2σ	P 0.75	2σ	P 0.75	2σ
As	$\mu g \cdot g^{-1}$	56	62	278	36	214	1138	161	89	201	240	92	118	67	88
Cd	$\mu g \cdot g^{-1}$	0.45	0.48	2.14	2.01	2.60	1.66	0.37	0.30	1.38	1.70	0.28	0.36	0.30	0.33
Cu	$\mu g \cdot g^{-1}$	53	61	1337	52	82	91	319	400	295	350	266	304	394	1167
Li	$\mu g \cdot g^{-1}$	75	82	–	–	–	–	145	125	194	286	126	166	79	201
Mo	$\mu g \cdot g^{-1}$	1.4	1.6	–	–	–	–	6.57	6.94	3.05	3.38	4.89	5.39	8.99	63.7
Sb	$\mu g \cdot g^{-1}$	12	13	–	–	32	12	0.63	0.84	0.29	0.33	0.57	0.74	0.88	0.97

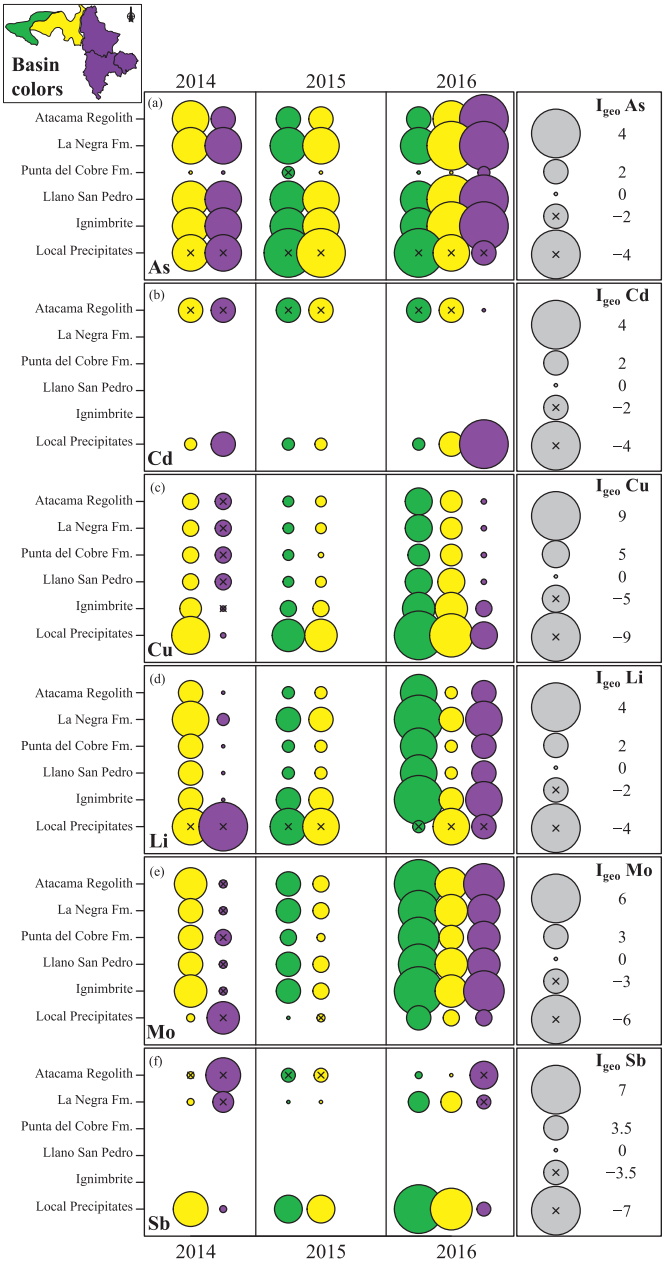

Fig. 6. Geo-accumulation index (I_{geo}) for selected elements. The materials used to calculate this index are: andesites to basaltic andesites of La Negra Formation (López, 2014; Oliveros et al., 2007), andesitic lavas of Punta del Cobre Formation (López, 2014), dacites of the Llano San Pedro volcanic complex (López, 2014), ignimbrites of dacitic composition (López, 2014), Atacama regolith from 30 cm depth (López, 2014), and chemical precipitates collected during this study from remote areas of the Andes.

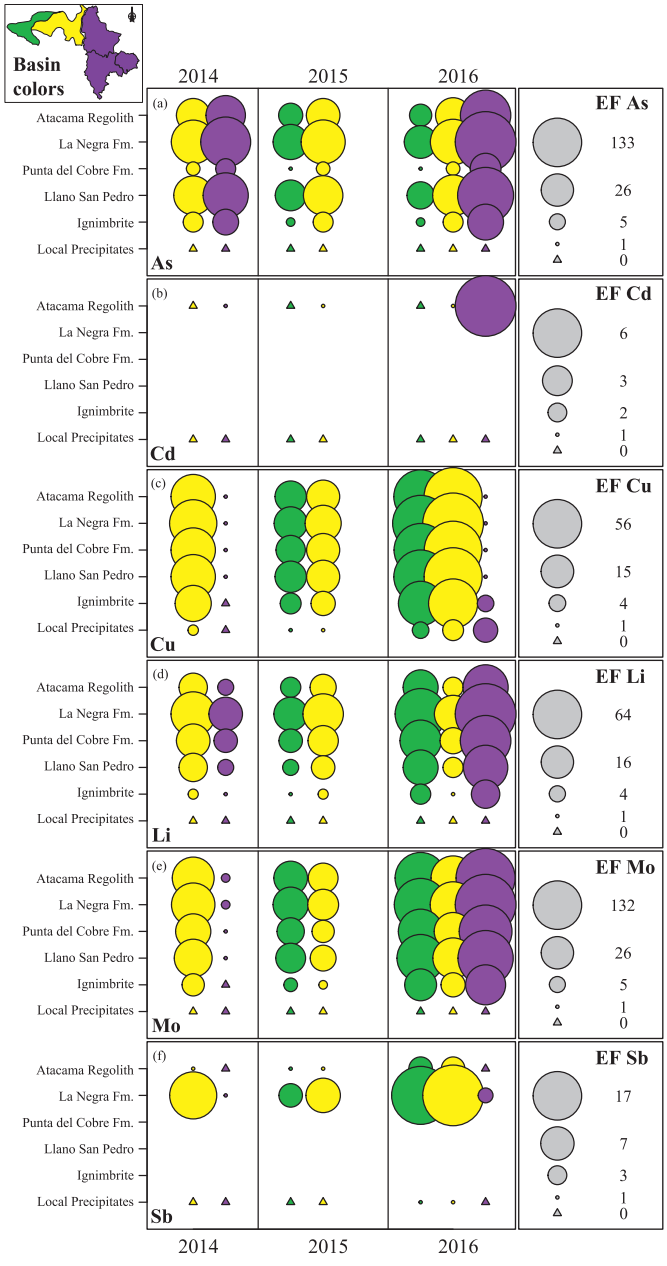

Fig. 7. Enrichment Factors (EFs) for selected elements. The materials used to calculate this index are: andesites to basaltic andesites of La Negra Formation (López, 2014; Oliveros et al., 2007), andesitic lavas of Punta del Cobre Formation (López, 2014), dacites of the Llano San Pedro volcanic complex (López, 2014), ignimbrites of dacitic composition (López, 2014), Atacama regolith from 30 cm depth (López, 2014), and chemical precipitates collected during this study from remote areas of the Andes.

In relation to probable sources, except for Cu, precipitates from the Andes could explain the high concentrations of the studied elements. However, the large distance between the basin and precipitates indicates that this material is not likely the source for elements in the El Salado Bajo Basin. Other rocks such as those found in the Punta del Cobre Formation, the Atacama regolith, and Ignimbrites could instead be the sources of As, Cd, Li and Sb (Fig. 7).

5. Discussion

Based on the conducted analyses, results obtained, and expected concentrations of each sample area, relevant observations, comparisons, and interpretations (such as possible sources) regarding the studied elements are summarized below in relation to the geology, anthropogenic activities, and geochemical anomalies (Section 5.1). A profile displaying the spatial variation of the average concentration of each of the studied elements at the sampling sites, between 2014 and 2016, is provided in Fig. 8 and the exact transect locations are shown in Fig. 2. Natural impacts on the redistribution of the studied elements is discussed in Section 5.2 and the temporal variation of concentration values at the sampling sites is highlighted as a function of the large-scale 2015 storm and flood event. Subsequently, applications to other similar environments are discussed in Section 5.3.

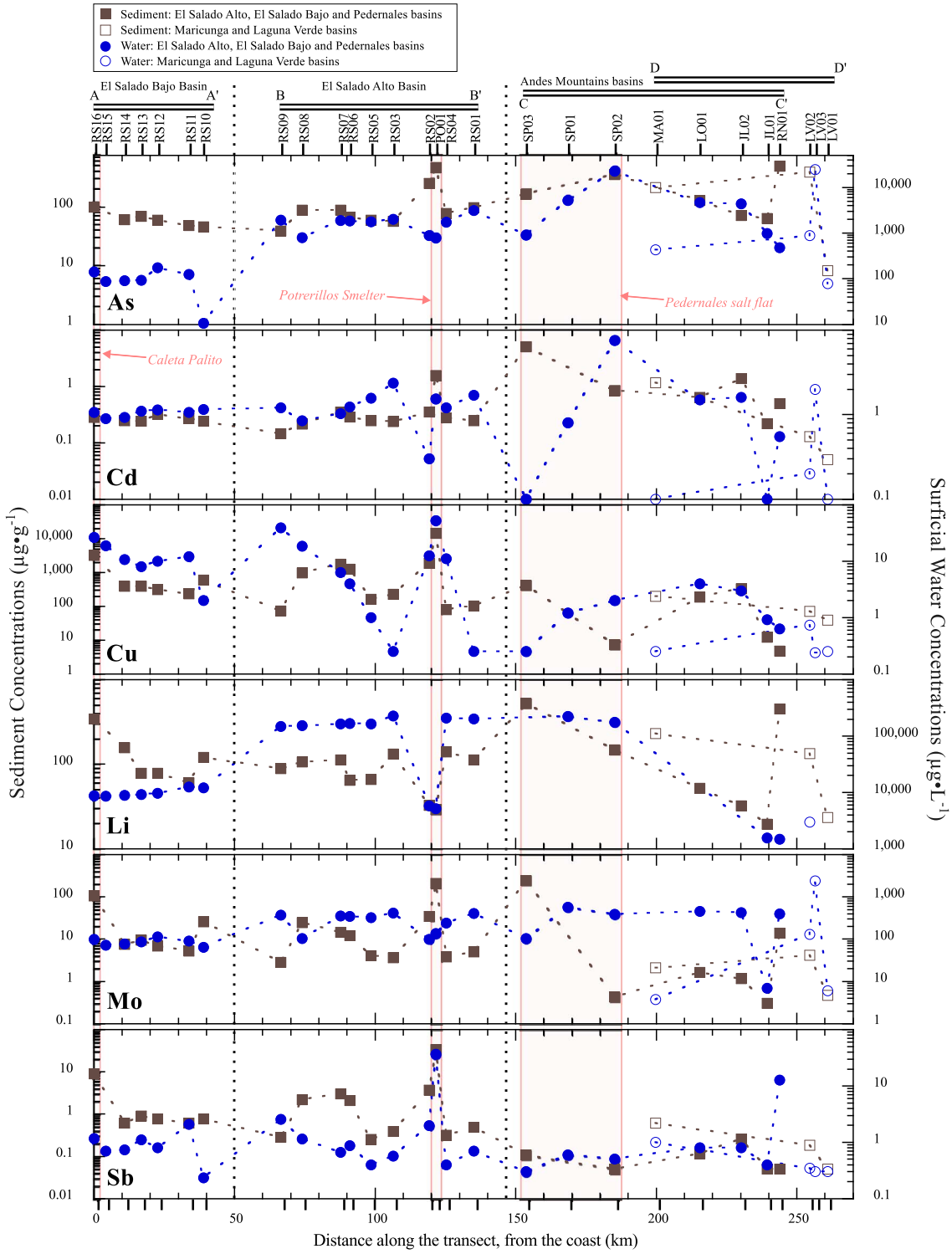

Fig. 8. Spatial distribution of average concentrations (2014 to 2016). Transect locations are provided in plan view in Fig. 2. For the Maricunga and Laguna Verde basins, due to their similar longitude and distinct latitude in relation to the Pedernales Basin, their symbols differ.

5.1. Geology, anthropogenic activities, and geochemical anomalies

5.1.1. Arsenic

The highest local geochemical background concentration for As in fluvial water and sediments is located in the Andes Mountains (Table 3) where the dominant geology corresponds to Cenozoic volcanic deposits and sedimentary sequences (Fig. 2d,e). Despite the fact that the As concentration is generally above the consulted regulations and recommendations for water and sediments (Figs. 4 and 5), in the studied basins, As is not considered a contaminant (Fig. 6a).

Increased natural concentrations of dissolved As in the Andes Mountains are a consequence of the presence of As-rich hot springs at Río Negro, Juncalito, and Laguna Verde (Aguirre and Clavero, 2000; Risacher et al., 1999; Tapia and Verdejo, 2015). Similar enrichments have also been observed at the El Tatio geysers, 500 km north of the study area. There, elevated concentrations provide an additional source

of dissolved As to the El Loa River (Romero et al., 2003).

High As local geochemical background concentrations are comparable to other mining sites worldwide (Oruro, Bolivia; Tapia et al., 2012; Tapia and Audry, 2013; Miedzianka, Poland; Gałuszka et al., 2015; Chalkidiki, Greece; Kelepertzis et al., 2010; Table 3b). However, in the case of the Northern Atacama Region, this local geochemical background is likely associated with natural sources of As present in large-scale evaporite belts of the Neogene Central Andes, which contain anomalous concentration of Li, As, Sr, and K (Alonso et al., 1991). Also, As is found in the Maricunga Metallogenic belt. This belt is rich in high-sulfidation gold deposits (Sillitoe et al., 1991) that are associated with elevated As concentrations (White and Hedenquist, 1995). In addition, and as determined in this study, precipitates from remote areas of the Andes and geologic formations similar to Punta del Cobre, a Jurassic to Cretaceous outcrop rich in andesites that bears the mineralization of the Inca de Oro District (Fig. 1a; Soto, 2010), are important sources of As for the Andes and El Salado Alto basins, respectively (Fig. 7a). It is also apparent from Fig. 8 that the concentration of As increases near the Potrerillos Smelter, attributable to the mining activities present there.

5.1.2. Cadmium

The highest local geochemical background of Cd concentration in fluvial water and sediments is found in the El Salado Alto and the Andes Mountains basins, respectively (Table 3). Despite the fact that this element is enriched when compared to fluvial water and sediment average global concentrations, in general it is not above water (Fig. 4) and sediment (Fig. 5) recommended values and is not considered a contaminant in any of the studied basins (Fig. 6b).

In relation to the origin of this element, in the Andes area, precipitates could be a source of Cd (Fig. 7b). In the El Salado Alto and Bajo basins, the Atacama Regolith might be an important source of Cd (Fig. 7b). It is also clear from Fig. 8 that the concentration of dissolved Cd is high in the eastern border of the Pedernales salt flat, and in sediments and water increases abruptly near the Potrerillos Smelter, attributable to the mining activities present there.

5.1.3. Copper

The highest local geochemical background concentration for Cu in fluvial water and sediments is found in El Salado Bajo Basin (Table 3). Copper concentrations are below national and international regulations for water (Fig. 4), yet Cu is importantly concentrated in sediments and is above the Canadian recommended values (Fig. 5). This element was classified as a contaminant in all the studied basins (Fig. 6c).

El Salado River is located in a well-known Cu-rich metallogenic province (Sillitoe, 2012; Sillitoe and Perelló, 2005) composed of Jurassic-Lower Cretaceous, Paleocene-Lower Eocene, and Upper Eocene-Lower Oligocene metallogenic belts (Fig. 1a). The Upper Eocene-Lower Oligocene and the Jurassic-Lower Cretaceous belts are recognized worldwide for the presence of large-scale porphyry Cu deposits (Sillitoe and Perelló, 2005) and IOCG deposits (Sillitoe, 2003), respectively.

Due to the Cu richness in this area, historically, the El Salado River has been significantly affected by mining activities, especially through the disposal of mining waste directly into the river over an approximate time period of 40 years (Castilla, 1983). This anthropogenic influence is evidenced by the fact that the highest elemental concentrations of Cu in fluvial water were found at the Potrerillos site during the three-year long sampling (Figs. 4 and 8). Additionally, sediments close to the Potrerillos Smelter and in the discharge area at Caleta Palito have the highest values of Cu (Fig. 8), supporting the idea that mining activities are an important source of anthropogenic Cu in the Northern Atacama Region.

Therefore it is likely that the natural presence of Cu-rich metallogenic belts, in addition to uncontrolled mining activities, have a direct relation to Cu contamination in the studied sediments.

5.1.4. Lithium

The highest local geochemical background concentration for Li in fluvial water is found in the Andes Mountains and El Salado Alto basins; for sediments, it is found in the Andes (Table 3). This element is above the recommended concentration for water as suggested by Aral and Vecchio-Sadus, 2008; (Fig. 4), and despite the fact that there are no regulations in Chile or Canada for its concentration in sediments, in this study it was found that Li is not considered a contaminant in any of the studied basins (Fig. 6d).

Dissolved Li concentrations are observed to be at their highest values in the Pedernales and El Salado Alto basins (Fig. 8). Brines from salt flats, in the Altiplano-Puna region, are known for their Li resources (Chong, 1988; Ericksen and Salas, 1990; Gajardo, 2014). In addition, Neogene Puna evaporites have anomalous concentrations of Li because of their closed drainages and position adjacent to the volcanic arc; thus, this basin can capture all the product of thermal activity there (Alonso et al., 1991). As suggested in this study, precipitates from remote areas of the Andes are also enriched in this element (Fig. 7d).

Therefore, the enrichment of Li in the Northern Atacama Region might be explained by natural sources of the Altiplano-Puna in addition to the transport of Li in fluvial water due to anthropogenic channelization of the Pedernales salt flat in the 1930s (Fig. 3a).

5.1.5. Molybdenum

Results from this study indicate that Mo presents the highest local geochemical background concentration for water in the Andes and El Salado Alto basins (Table 3a), and for sediments, the highest local geochemical background is present in the El Salado Bajo Basin (Table 3b). In water, for > 60% of the collected samples, the concentration of Mo is above the WHO recommendation (Fig. 4). Additionally, Mo is considered a contaminant in sediments of El Salado Alto and El Salado Bajo basins (Fig. 6e).

Natural high concentration of dissolved Mo has been found in groundwater from the Spence porphyry Cu deposit (Leybourne and Cameron, 2008), and as determined in this study, the highest local geochemical background for Mo in fluvial water is in the Andes and El Salado Alto basins (Fig. 8). Thus, natural Mo-rich brines and porphyry copper deposits related groundwater could be the source for Mo in water.

In the case of sediments, the highest local geochemical background of Mo is in El Salado Bajo Basin. The precipitates from remote areas of the Andes do not explain the high concentration of this element as do other rocks of the Chañaral Basin (Fig. 7e). Due to the fact that Mo is strongly correlated to Cu (Table 4), it is assumed that it originates from the processing of porphyry Cu-Mo deposits, suggesting an anthropogenic source for Mo in sediments. Therefore, Mo shows a geogenic origin in fluvial water and an anthropogenic origin in sediments.

5.1.6. Antimony

The highest local geochemical background concentration for Sb is present in El Salado Bajo Basin for fluvial water and sediments (Table 3). This element presents < 11% of water samples above the US EPA and WHO recommendations and any of these sample locations are in El Salado Bajo Basin (Fig. 4). In the case of sediments, there are no guidelines for Sb, however in this study it was shown that Sb is considered a contaminant in the El Saldo Bajo Basin (Fig. 6f).

In a similar manner to Cu, this element shows the highest values for fluvial water and sediments in the Potrerillos site (Figs. 4, 5, and 8). This is strongly correlated to Cu and Mo (Table 4), suggesting that mining activities could be the most important source for Sb in fluvial water and sediments of the El Salado River.

5.2. Natural element redistribution

Based on Table 4, all studied elements present strong positive correlations in the El Salado Alto and El Salado Bajo basins, except for Li in

Table 4
Correlation coefficients between elements of surface water (a) and fluvial sediments (b).

(a) Water

	All samples of Northern Atacama Region					Andes					El Salado Alto					El Salado Bajo				
	As	Cd	Cu	Li	Mo	As	Cd	Cu	Li	Mo	As	Cd	Cu	Li	Mo	As	Cd	Cu	Li	Mo
Cd	0.67					0.76					0.35					0.69				
Cu	− 0.19	0.04				0.01	0.14				− 0.35	0.04				0.70	0.54			
Li	0.34	0.48	− 0.07			0.69	0.56	0.74			− 0.89	− 0.21	− 0.67			− 0.68	− 0.90	− 0.84		
Mo	0.74	0.26	− 0.16	0.88		0.73	0.19	− 0.04	0.94		0.87	0.29	− 0.35	0.94		0.87	0.94	0.61	− 0.90	
Sb	− 0.08	0.01	0.55	− 0.18	0.01	− 0.19	− 0.06	− 0.15	− 0.10	0.15	− 0.21	0.00	0.67	− 0.72	− 0.22	0.76	0.64	0.55	− 0.85	0.71

(b) Sediments

	All samples of Northern Atacama Region					Andes					El Salado Alto					El Salado Bajo				
	As	Cd	Cu	Li	Mo	As	Cd	Cu	Li	Mo	As	Cd	Cu	Li	Mo	As	Cd	Cu	Li	Mo
As	0.18					− 0.03					0.87					0.18				
Cd	0.44	0.09				− 0.06	0.62				0.88	0.97				0.85	− 0.07			
Cu	0.14	0.30	0.05			0.27	0.37	0.28			− 0.51	− 0.37	− 0.43			0.75	− 0.20	0.97		
Li	0.29	0.81	0.52	0.46		0.00	0.95	0.52	0.49		0.91	0.96	0.99	− 0.43		0.82	0.00	0.97	0.91	
Mo	0.44	0.06	0.99	0.08	0.51	0.27	− 0.08	0.19	0.21	− 0.21	0.88	0.97	0.99	− 0.42	0.99	0.90	− 0.01	0.99	0.94	0.96

the El Salado Alto Basin and Cd in the El Salado Bajo Basin. These correlations suggest that besides mining there are likely other controls on the redistribution of elements.

5.2.1. Redistribution in the Andes Mountains

From the collected data, there was a systematic increase in the average concentration of dissolved Cu, Sb, and Mo. Concentrations of As and Cd remained constant. In fluvial sediments, the average concentration of all analyzed elements increased in 2016. Comparing specific sites (RN01 and SP02), there is a clear increase of Mo and Sb in the dissolved fraction however this is not observed for Cu. With respect to fluvial sediments, specific sites (LV01, LV02, JL02, LO01) showed a marked increase in Cu and Mo concentrations (contaminants of the El Salado Alto Basins), followed by Li and As, and to a lesser extent Cd and Sb. In 2016, saline precipitate samples from Pedernales (SP02-C; 3361 m a.s.l.) and Río Negro (RN01; 4118 m a.s.l.) showed a yellow coloration that was not present in 2014. These samples have the highest concentrations of As and Li in all the surveyed basins (Fig. 3e and f).

With the initiation of the March 2015 mudflow, recent research indicates that snow covered a wide area above 3600 m a.s.l. (Jordan et al., 2015; Fig. 1c), which is in agreement with information from local border agents in the field (personal communication, 2015). Studies performed in Scotland have demonstrated that there is an increase in concentration of dissolved Al, Cd, Cu, Fe, Mn, and Pb after snow melt (Abrahams et al., 1989). Previous research in the Arctic has additionally shown that polar environments are especially sensitive to these types of changes, of which, some would have direct effects on the role of snow in contaminant scavenging (Macdonald et al., 2005). The Desert Andes are characterized by permanent snow patches and small glaciers (Lliboutry, 1988). Therefore it is suggested that snow cover, above 3600 m a.s.l., and subsequent melting could have played an important role in the transport of elements from the west (the Cu-Mo rich metallogenic belt). This transport would have acted as a catalyst increasing the concentrations of Cu, Mo, and Sb in the dissolved fraction and Cu, Mo and (to a lesser extent) Li, As, Cd and Sb in fluvial sediments. Transport could have also produced enrichment of As and Li in saline crusts within the Andes Mountains of the Northern Atacama Region.

5.2.2. Redistribution in the El Salado Alto basin

From 2014 to 2015, the El Salado Alto Basin experienced a dilution in Cd, Cu, and Sb concentrations; this effect was not observed for As and Mo (Fig. 4). For Cu and Sb, the highest values were always found in Potrerillos (Fig. 4). Intense rainfall in the El Salado Alto Basin (80 mm; MOP, 2017) diluted these elements, diminishing their concentration in the dissolved fraction. As previously proposed, dissolved As and Mo originate in the Andes Mountains and the Altiplano-Puna plateau. Any increase in their concentration is related to the transport of these elements from their source area. For Cd, dilution is more complex. Although, in general, the highest concentrations of particulate and dissolved Cd are found in the Andes Mountains, this was not the case in 2014 when the highest Cd concentration found in the El Salado Alto Basin was at Potrerillos (Fig. 4). This suggests that dilution of this source caused the decreased concentrations in 2015. In the El Salado Alto Basin, most elements (As, Cu, Li, Mo, and Sb) in fluvial sediments show decreases in concentration in 2015 (Fig. 5), which is likely related to transport downstream during the flooding (Jordan et al., 2015; Wilcox et al., 2016).

5.2.3. Redistribution in the El Salado Bajo basin

Despite the redistribution of elements in the Andes Mountains and El Salado Alto Basin, the most notable changes of this type occur in the El Salado Bajo Basin. Dissolved elements from El Salado Bajo show higher concentrations of As, Cd, Cu, Mo, and Sb just after the 2015 storm and mudflow, with the lowest values in 2014 (Fig. 4). A possible explanation for this phenomenon is that, during 2014, the El Salado

Alto Basin was not hydrologically connected to the El Salado Bajo Basin, but rather the surface water flow ended 10 km west of Diego de Almagro (Fig. 1a). In 2015, the El Salado Alto, Chañaral and El Salado Bajo basins became connected hydrologically due to the El Salado River flood. This connection was observed two months after the flooding during the field campaign, that is, surficial flow with a notable amount of suspended matter at locations between Diego de Almagro and the first site of the El Salado Bajo Basin (Fig. 2b).

In spite of the pronounced 2015 storm event, hydrologic conditions reverted in 2016 as the El Salado Alto Basin terminated 20 km east of Diego de Almagro (Fig. 1a and Fig. 2c; water not present at RS08 and RS09), and furthermore, as in 2014, surficial water of the El Salado Alto Basin was not connected to the Chañaral and El Salado Bajo Basins. These normal conditions where water of the El Salado Alto and El Salado Bajo basins were confined to their respective areas, as of 2016, is capable of explaining the decrease in analyzed element concentrations when compared to those of 2015 (Fig. 4). For sediments collected in 2016, available samples show that Li, Mo, Cu, and Sb represent respectively, 7, 5, 4, and 3 times the 2015 concentrations. Arsenic and Cd do not exhibit significant changes in concentration at these sites (Fig. 5).

5.3. The case of copper and applications to other dry areas of the world

5.3.1. Copper in the El Salado Alto and El Salado Bajo basins

Large-scale porphyry copper deposits and mining activities are scattered throughout the El Salado Alto and El Salado Bajo basins. Average dissolved concentrations of Cu were 10, 42, and 27 μg L^{-1} in 2014, 2015, and 2016 respectively, which is approximately 6 times greater than the worldwide average for riverine Cu (Table 1; Gaillardet et al., 2003) as well as approximately 2 orders of magnitude lower than the concentration recommended for safe drinking water (Table 1; NCH 409, 2006; US EPA, 2009; WHO, 2011). Maximum concentrations for dissolved Cu were found at the Potrerillos stream and were 59, 48, and 50 μg L^{-1} in 2014, 2015, and 2016 respectively (Figs. 4 and 8).

Previous studies at Caleta Palito (Figs. 1a and 3b) showed an increased concentration of dissolved Cu in the disposal channel, of 2390 μg L^{-1} (Castilla, 1996). During the field campaigns of this study, values obtained at the same site are 2 orders of magnitude lower than previously reported. An explanation for these large differences could be the construction of the Pampa Austral tailing dam in the late 1990s, which helped to control and restrict concentrations of dissolved Cu entering the main stream. No important changes in concentrations of dissolved Cu were observed in studies with pH ≥ 6 (Atkinson et al., 2007). Therefore, these lower than expected values are reasonable because the El Salado Alto and El Salado Bajo basins were characterized by circumneutral to alkaline pH values thereby preventing the dissolution of Cu in the basins and sampling years of this study. Furthermore, the presence of carbonate rocks is limited to the Jurassic marine sequences which are found in the headwaters (RS01; Fig. 2c) as well as to the west of Diego de Almagro (sites RS09 to RS10; Figs. 2b,c), therefore, this type of rock is probably not controlling pH. Additionally, Leybourne and Cameron (2008) determined that in the Spence porphyry copper deposit, under circumneutral pH and high salinity conditions similar to those found in the present study (Aguirre and Clavero, 2000; Risacher et al., 1999), the concentrations of porphyry copper deposit-associated metal and metalloid species in groundwater are stable in solution for relatively long transport distances (> 1 km) in contrast to Cu which complexes as a cation (< 1 km). In the studied sites, it was found that dissolved and particulate Cu and Sb have elevated concentrations in the vicinity of Potrerillos. However, the same result was not reported downstream or in the Andes, suggesting that Cu and Sb complex as cations in the proximity of their source location. On the contrary, As and Mo migrate downstream long distances from their source. Considering average pH (8.6) and Eh (− 0.09 V) conditions during the 2016 sampling campaign as well as Eh-pH diagrams for aqueous As (Smedley and Kinniburgh, 2002) and Mo (Anbar, 2004), it is inferred that these elements are transported as $HAsO_4^{2-}$ and MoO_4^{2-}, respectively.

5.3.2. Applications to other dry areas of the world

Consequences of the exploitation of Cu have been studied in select locations of the Atacama Desert, Chile (Castilla, 1983, 1996; Ramírez et al., 2005). Nevertheless, at present there are other similar dry regions in which porphyry copper deposits are exploited. One of these locations is the Oyu Tolgoi porphyry Cu-Au-Mo deposit located in the southern part of the Gobi Desert, Mongolia. Modern exploration of this area started in the 1980s, and the first copper concentrate was produced and exported in 2013 (Porter, 2016), resulting in an improvement of their economy (The World Bank, 2017). The Gobi region is a cold desert and a snow cover is formed between November and February (Batima et al., 2005). As shown from this study, snowmelt can facilitate the remobilization of contaminant elements in this type of environment especially if mining activities are unregulated.

Likewise, Iran is related to the central Iranian volcano-plutonic Cu belt in which the Sarcheshmeh porphyry deposit is located, the most important Cu-Mo mine in Iran (Atapour and Aftabi, 2007). This mine is located 60 km NW from Kerman, the nearest city, and the Sarcheshmeh Cu smelter plant started operations in 1981. Conducted studies close to this facility have shown that mining activities have resulted in soil contamination (Khorasanipour and Aftabi, 2011). At Sarcheshmeh, the average annual precipitation varies from 300 to 550 mm, the temperature ranges from + 35 °C to − 20 °C, and the area is covered with snow 3 to 4 months per year (Ardejani et al., 2008). Generally, rainfall in Iran occurs from January to April (Weather Online, 2017); however, in a similar manner to the Atacama Desert, recently in August 2017, a vast area of northern Iran approximately 500 km north of Kerman was affected by heavy rains and flash floods, resulting in at least 12 fatalities, 2 missing people, and over 2000 affected individuals (Davies, 2017). As illustrated in this study, remobilization of mining-related contaminants could also occur in this arid to semiarid environment due to flash floods or snow melt.

6. Conclusions

Analyses of surface water and fluvial sediments of the Northern Atacama Region of Chile, as presented herein, have aided in the assessment of the main regional contaminants and probable sources, the establishment of a local geochemical background, and the assessment of the redistribution of contaminant elements as a result of the large-scale March 2015 Atacama flood event and mudflow. This analysis and evaluation aids in the goal of better understanding contaminant sources and impacts due to natural and anthropogenic factors in regions with scarce water resources.

In regard to the central subjects of this study, the following conclusions are summarized below and could be applicable to other similar geologic and hydrologic systems outside of the immediate research area:

6.1. Sources and contaminant elements

Samples obtained in the Northern Atacama Region indicate that Li, As, Mo, Cd, Sb, and Cu all exhibit higher concentrations in surface water and fluvial sediments when compared to worldwide averages in rivers and the UCC, respectively. In particular, concentrations of Li, As, and Mo are orders of magnitude greater in surface water when compared to worldwide averages in rivers. Despite elemental enrichment in the analyzed dissolved load samples, it is concluded that dissolved As, Cd, Li, and Mo originate from natural sources, whereas dissolved Cu and Sb are considered mining-related contaminants. In the particulate fraction, it is inferred that As, Li, and Cd enrichment is natural, originating from salt flats, Neogene evaporites, and epithermal deposits of

the Andes Mountains. Nevertheless, enrichment in Cu, Mo, and Sb is related to fluvial contamination from mining activities. The obtained local geochemical background is mainly reflecting geology for As, Cd and Li in fluvial water and sediments, however this is not concluded for Cu, Mo and Sb which reflect the combination of anthropogenic activities and geology. When comparing concentrations in surface water and sediments from the Northern Atacama Region to other sites impacted by mining activities such as Oruro, Bolivia, of the studied elements, only Sb exhibits higher values in the dissolved fraction outside of the studied region while concentrations in sediments are comparable. Aside from natural enrichment and human-induced contamination, remobilization of elements has occurred as the result of floods and snowmelt in the El Salado River basins (El Salado Alto and El Salado Bajo) and Andes Mountain basins, respectively.

6.2. March 2015 Flooding

In the Andes Mountains, the March 2015 massive flood event spurred an increase of Cu, Mo and Sb in the dissolved fraction as well as an increase of Cu, Mo, and, to a lesser extent, Li, As, Cd and Sb in fluvial sediments. Flooding also led to an enrichment of As and Li in saline crusts of the Andes Mountains. From 2014 to 2015, the El Salado Alto Basin samples exhibited a dilution of dissolved concentrations in Cd, Cu, and Sb due to increased precipitation. A major portion of the analyzed elements in the particulate fraction decreased in concentration just after the event and subsequently increased 1 year after the flood. The El Salado Bajo Basin showed the most significant changes in concentration in the dissolved fraction. Just after the 2015 event, concentrations increased due to the creation of a hydrologic connection between the El Salado Alto and El Salado Bajo basins.

6.3. Copper

Despite the fact that this region has been affected by intense mining activities, concentrations of Cu in the dissolved fraction are lower than previously reported. This is likely related to circumneutral to alkaline pH and the complexation of Cu as a cation.

Acknowledgements

This survey would not be possible without the economic support provided by a grant from the Universidad de Antofagasta, the use of laboratory facilities provided by Domingo Román, Pedro Cortés, and Juan Ávila of the Chemistry Department and Jorge Valdés and Sue Ellen Vega from the Instituto de Investigaciones Oceanológicas, at the Universidad de Antofagasta. We thank Verónica Oliveros for providing unpublished data of As, Mo, and Sb of La Negra Formation and two anonymous reviewers for their valuable suggestions and contributions. In addition we appreciate the help of Sergio Villagrán during the sampling campaigns, Stephane Audry during the 2014 sampling campaign, and the GET laboratory during water sample analyses of 2014. We would also like to thank undergraduate students Francisca Verdejo and Carlos Acuña (Universidad Católica del Norte). The March 2016 sampling campaign was funded by a grant entitled Programa de Inserción en la Academia (PAI) 79150070.

References

Abrahams, P.W., Tranter, M., Davies, T.D., Blackwood, I.L., 1989. Geochemical studies in a remote Scottish upland catchment II. Streamwater chemistry during snow-melt. Water Air Soil Pollut. 43, 231–248. http://dx.doi.org/10.1007/BF00279194.

Aguirre, I., Clavero, J., 2000. Antecedentes Fisicoquímicos Preliminares de Cuerpos de Agua Superficial del Altiplano de la III Región de Atacama, Chile, in: Sesión Temática 1. Presented at the IX Congreso Geológico Chileno, Puerto Varas, Chile. pp. 1–5.

Alonso, R.N., Jordan, T.E., Tabbutt, K.T., Vandervoort, D.S., 1991. Giant evaporate belts of the Neogene central Andes. Geology 19, 401–404. http://dx.doi.org/10.1130/0091-7613(1991)019<0401:GEBOTN>2.3.CO;2.

Anbar, A., 2004. Molybdenum stable isotopes: observations, interpretations and directions|reviews in mineralogy and geochemistry. Rev. Mineral. Geochem. 55, 429–454. http://dx.doi.org/10.2138/gsrmg.55.1.429.

Aral, H., Vecchio-Sadus, A., 2008. Toxicity of lithium to humans and the environment—a literature review. Ecotoxicol. Environ. Saf. 70, 349–356. http://dx.doi.org/10.1016/j.ecoenv.2008.02.026.

Ardejani, F., Karami, G., Assadi, A., Dehghan, R., 2008. Hydrogeochemical investigations of the Shour River and groundwater affected by acid mine drainage in Sarcheshmeh porphyry copper mine. In: Preceedings 2008 Mine Water and the Environment. Presented at the 10th International Mine Water Association Congress, Karlsbad, Czech Republic, pp. 235–238.

Atapour, H., Aftabi, A., 2007. The geochemistry of gossans associated with Sarcheshmeh porphyry copper deposit, Rafsanjan, Kerman, Iran: implications for exploration and the environment. J. Geochem. Explor. 93 (1), 47–65.

Atkinson, C.A., Jolley, D.F., Simpson, S.L., 2007. Effect of overlying water pH, dissolved oxygen, salinity and sediment disturbances on metal release and sequestration from metal contaminated marine sediments. Chemosphere 69, 1428–1437. http://dx.doi.org/10.1016/j.chemosphere.2007.04.068.

Batima, P., Natsagdorj, L., Gombluudev, P., Erdenetsetseg, B., 2005. Observed climate change in Mongolia. In: AIACC Working Papers. 12. pp. 1–26. http://www.start.org/Projects/AIACC_Project/working_papers/Working%20Papers/AIACC_WP_No013.pdf.

Benavides, J., Kyser, T.K., Clark, A.H., Oates, C.J., Zamora, R., Tarnovschi, R., Castillo, B., 2007. The Mantoverde iron oxide-copper-gold district, III Región, Chile: the role of regionally derived, nonmagmatic fluids in chalcopyrite mineralization. Econ. Geol. 102, 415–440. http://dx.doi.org/10.2113/gsecongeo.102.3.415.

Biblioteca Nacional de Chile, 2017. “Mineral de potrerillos”, en: Origen de la Gran Minería del Cobre (1904–1930) www.memoriachilena.cl (web archive link, 17 January 2017). URL http://www.memoriachilena.cl/602/w3-article-96522.html (accessed 1.17.17).

Canadian Council of Ministers of the Environment, 2001. Canadian Sediment Quality Guidelines for the Protection of Aquatic Life. Environment Canada Guidelines and Standards Division, Canada.

Castilla, J.C., 1983. Environmental impact in sandy beaches of copper mine tailings at Chañaral. Chile. Mar. Pollut. Bull. 14, 459–464. http://dx.doi.org/10.1016/0025-326X(83)90046-2.

Castilla, J.C., 1996. Copper mine tailing disposal in northern Chile rocky shores: *Enteromorpha compressa* (Chlorophyta) as a sentinel species. Environ. Monit. Assess. 40, 171–184. http://dx.doi.org/10.1007/BF00414390.

Chen, C.-W., Kao, C.-M., Chen, C.-F., Dong, C.-D., 2007. Distribution and accumulation of heavy metals in the sediments of Kaohsiung Harbor, Taiwan. Chemosphere 66, 1431–1440. http://dx.doi.org/10.1016/j.chemosphere.2006.09.030.

Chong, G., 1988. The Cenozoic saline deposits of the Chilean Andes between 18°00′ and 27°00′ south latitude. In: Bahlburg, D.H., Breitkreuz, P.D.D.C., Giese, P.D.P. (Eds.), The Southern Central Andes, Lecture Notes in Earth Sciences. Springer, Berlin Heidelberg, pp. 137–151. http://dx.doi.org/10.1007/BFb0045179.

Clarke, J.D.A., 2006. Antiquity of aridity in the Chilean Atacama Desert. Geomorphology 73, 101–114. http://dx.doi.org/10.1016/j.geomorph.2005.06.008.

COCHILCO, 2016. Franjas Metalogénicas de los Andes Centrales: Blancos Clave Para la Exploración Minera.

Contreras, J.P., Ramírez, C., Garrido, N., Núñez, G., 2015. Caracterización hídrica y geológica de los aluviones del 25 y 26 de marzo de 2015 en la cuenca del Río El Salado, Región de Atacama, Chile. In: Geología Para El Siglo XXI. Presented at the XIV Congreso Geológico Chileno, La Serena, Chile, pp. 785–788.

Cornejo, P., Tosdal, R.M., Mpodozis, C., Tomlinson, A.J., Rivera, O., Fanning, C.M., 1997. El Salvador, Chile porphyry copper deposit revisited: geologic and geochronologic framework. Int. Geol. Rev. 39, 22–54. http://dx.doi.org/10.1080/00206819709465258.

Davies, R., 2017. Iran – 12 killed in flash floods in North – FloodList, floodlist.com (web archive link, 13 August 2017). http://floodlist.com/asia/iran-flash-floods-august-2017, Accessed date: 5 October 2017.

DGA, 2014. Simposio Avances y Desafíos en la Problemática del Arsénico en Aguas de Chile y el Mundo.

Earle, L.R., Warner, B.G., Aravena, R., 2003. Rapid development of an unusual peat-accumulating ecosystem in the Chilean Altiplano. Quat. Res. 59, 2–11. http://dx.doi.org/10.1016/S0033-5894(02)00011-X.

EN ISO 17294-2, 2016. Water Quality - Application of Inductively Coupled Plasma Mass Spectrometry (ICP-MS) - Part 2: Determination of Selected Elements Including Uranium Isotopes.

Ericksen, G.E., Salas, R., 1990. Geology and Resources of Salars in the Central Andes.

Espinoza, S., 1990. The Atacama-Coquimbo Ferriferous Belt, Northern Chile. In: Fontboté, P.D.L., Amstutz, P.D.G.C., Cardozo, P.D.M., Cedillo, P.D.E., Frutos, P.D.J. (Eds.), Stratabound Ore Deposits in the Andes, Special Publication No. 8 of the Society for Geology Applied to Mineral Deposits. Springer Berlin Heidelberg, pp. 353–364.

Gaillardet, J., Viers, J., Dupré, B., 2003. 5.09 - trace elements in river waters. In: Turekian, H.D.H.K. (Ed.), Treatise on Geochemistry. Pergamon, Oxford, pp. 225–272.

Gajardo, A., 2014. Potencial de Litio en Salares del Norte de Chile.

Gałuszka, A., Migaszewski, Z.M., Dołęgowska, S., Michalik, A., Duczmal-Czernikiewicz, A., 2015. Geochemical background of potentially toxic trace elements in soils of the historic copper mining area: a case study from Miedzianka Mt., Holy Cross Mountains, south-central Poland. Environ. Earth Sci. 74, 4589–4605. http://dx.doi.org/10.1007/s12665-015-4395-6.

Hauser, A., 1997a. Catastro y Caracterización de las Fuentes de Aguas Minerales y Termales de Chile.

Hauser, A., 1997b. Los Aluviones del 18 de Junio de 1991 en Antofagasta: un Análisis Crítico, a 5 Años del Desastre. SERNAGEOMIN, Santiago.

International Mining, 2016. High-arsenic copper concentrates. www.im-mining.com (web archive link, 23 February 2016). http://im-mining.com/2016/02/23/high-arsenic-

copper-concentrates/, Accessed date: 9 May 2017.
ISO 15587-1, 2002. Water Quality - Digestion for the Determination of Selected Elements in Water - Part 1: Aqua Regia Digestion.
Jordan, T., Riquelme, R., González, G., Herrera, C., Godfrey, L., Colucci, S., Gironás, J., Gamboa, C., Urrutia, J., Tapia, L., Centella, K., Ramos, H., 2015. Hydrological and geomorphological consequences of the extreme precipitation event of 24–26 March 2015, Chile. In: Geología Para El Siglo XXI. Presented at the XIV Congreso Geológico Chileno, La Serena, Chile, pp. 777–780.
Kelepertzis, E., Argyraki, A., Daftsis, E., Ballas, D., 2010. Quality characteristics of surface waters at Asprolakkas river basin, N.E. Chalkidiki, Greece. Bull. Geol. Soc. Greece 1–10.
Khorasanipour, M., Aftabi, A., 2011. Environmental geochemistry of toxic heavy metals in soils around Sarcheshmeh porphyry copper mine smelter plant, Rafsanjan, Kerman, Iran. Environ. Earth Sci. 62 (3), 449–465.
Leybourne, M.I., Cameron, E.M., 2008. Source, transport, and fate of rhenium, selenium, molybdenum, arsenic, and copper in groundwater associated with porphyry–Cu deposits, Atacama Desert, Chile. Chem. Geol. 247, 208–228. http://dx.doi.org/10.1016/j.chemgeo.2007.10.017.
Lliboutry, L., 1988. Glaciers of Chile and Argentina, glaciers of the Dry Andes. In: Satellite Image Atlas of Glaciers of the World, South America, Professional Paper United States Geological Survey, pp. 109–147.
López, L.F., 2014. Exploraciones Geoquímicas de Yacimientos Bajo Cobertura Transportada en el Distrito de Inca de Oro, Atacama, Chile: Evolución de Regolito y Paisaje e Impactos en Métodos Geoquímicos Indirectos (Magíster en Ciencias Mención Geología). Universidad de Chile, Santiago.
Macdonald, R.W., Harner, T., Fyfe, J., 2005. Recent climate change in the Arctic and its impact on contaminant pathways and interpretation of temporal trend data. Sci. Total Environ. 342, 5–86. Sources, Occurrence, Trends and Pathways of Contaminants in the Arctic Bidleman SI. https://doi.org/10.1016/j.scitotenv.2004.12.059.
Matschullat, J., Ottenstein, R., Reimann, C., 2000. Geochemical background – can we calculate it? Environ. Geol. 39, 990–1000. http://dx.doi.org/10.1007/s002549900084.
MOP, 2017. Servicios Hidrometeorológicos. Minist. Obras Públicas - Dir. Gen. Aguas. http://www.dga.cl/productosyservicios/servicioshidrometeorologicos/Paginas/default.aspx, Accessed date: 16 January 2017.
Muller, G., 1979. Schwermetalle in den Sedimenten des Rheins - Veränderungen seit. Umschau 79, 778–783.
NCH 409, 2006. NCH 409/1 Norma Calidad del Agua Potable, NCH. 409. pp. 1.
Neary, D., García-Chevesich, P., 2008. Hydrology and erosion impacts of mining derived coastal sand dunes, Chañaral Bay, Chile. Hydrology and Water Resources in Arizona and the Southwest. 38. pp. 47–52.
Nowrouzi, M., Pourkhabbaz, A., 2014. Application of geoaccumulation index and enrichment factor for assessing metal contamination in the sediments of Hara Biosphere Reserve, Iran. Chem. Speciat. Bioavailab. 26, 99–105. http://dx.doi.org/10.3184/095422914X13951584546986.
Oliveros, V., Morata, D., Aguirre, L., Féraud, G., Fornari, M., 2007. Magmatismo asociado a subducción del Jurásico a Cretácico Inferior en la Cordillera de la Costa del norte de Chile (18°30′–24°S): geoquímica y petrogenesis. Rev. Geol. Chile 34, 209–232. http://dx.doi.org/10.4067/S0716-02082007000200003.
Olson, S., 1989. The stratigraphic and structural setting of the Potrerillos porphyry copper district, Northern Chile. Rev. Geológica Chile 16, 3–39.
Porter, T.M., 2016. The geology, structure and mineralisation of the Oyu Tolgoi porphyry copper-gold-molybdenum deposits, Mongolia: a review. Geosci. Front. 7 (3), 375–407.
Ramírez, M., Massolo, S., Frache, R., Correa, J.A., 2005. Metal speciation and environmental impact on sandy beaches due to El Salvador copper mine, Chile. Mar. Pollut. Bull. 50, 62–72. http://dx.doi.org/10.1016/j.marpolbul.2004.08.010.
Rioseco, R., Tesser, C., 2016. Cartografía interactiva de los climas de Chile: antecedentes generales. http://www7.uc.cl/sw_educ/geografia/cartografiainteractiva/Inicio/Paginas/UntitledFrameset-1.htm, Accessed date: 9 May 2016.
Risacher, F., Alonzo, H., Salazar, C., 1999. Geoquímica de Aguas en Cuencas Cerradas: I, II y III regiones - Chile.
Risacher, F., Alonso, H., Salazar, C., 2003. The origin of brines and salts in Chilean salars: a hydrochemical review. Earth-Sci. Rev. 63, 249–293. http://dx.doi.org/10.1016/S0012-8252(03)00037-0.
Romero, L., Alonso, H., Campano, P., Fanfani, L., Cidu, R., Dadea, C., Keegan, T., Thornton, I., Farago, M., 2003. Arsenic enrichment in waters and sediments of the Rio Loa (Second Region, Chile). Appl. Geochem. 2001 (18), 1399–1416. Arsenic Geochemistry-selected papers from the 10th Water-Rock Interaction Symposium, Villasimius, Italy, 10–15 June. https://doi.org/10.1016/S0883-2927(03)00059-3.
Rudnick, R.L., Gao, S., 2003. 3.01 - composition of the continental crust. In: Turekian, H.D.H.K. (Ed.), Treatise on Geochemistry. Pergamon, Oxford, pp. 1–64.
Schnurr, W.B.W., Trumbull, R.B., Clavero, J., Hahne, K., Siebel, W., Gardeweg, M., 2007. Twenty-five million years of silicic volcanism in the southern central volcanic zone of the Andes: geochemistry and magma genesis of ignimbrites from 25 to 27°S, 67 to 72°W. J. Volcanol. Geotherm. Res. 166, 17–46. http://dx.doi.org/10.1016/j.jvolgeores.2007.06.005.
Sillitoe, R.H., 1997. Characteristics and controls of the largest porphyry copper-gold and epithermal gold deposits in the circum-Pacific region. Aust. J. Earth Sci. 44, 373–388. http://dx.doi.org/10.1080/08120099708728318.
Sillitoe, R.H., 2003. Iron oxide-copper-gold deposits: an Andean view. Mineral. Deposita 38, 787–812. http://dx.doi.org/10.1007/s00126-003-0379-7.
Sillitoe, R., 2012. Copper provinces. Soc. Econ. Geol. Publ. 16, 1–18 Special Publication No.
Sillitoe, R., Perelló, J., 2005. Andean copper province: tectonomagmatic settings, deposit types, metallogeny, exploration, and discovery. Econ. Geol. 845–890 100th Anniversary Volume.
Sillitoe, R.H., McKee, E.H., Vila, T., 1991. Reconnaissance K-Ar geochronology of the Maricunga gold-silver belt, northern Chile. Econ. Geol. 86, 1261–1270. http://dx.doi.org/10.2113/gsecongeo.86.6.1261.
Smedley, P.L., Kinniburgh, D.G., 2002. A review of the source, behaviour and distribution of arsenic in natural waters. Appl. Geochem. 17, 517–568. http://dx.doi.org/10.1016/S0883-2927(02)00018-5.
SONAMI Estadísticas de producción de cobre, oro, plata, molibdeno y combustibles, www.sonami.cl (web archive link, 2017). http://www.sonami.cl/site/estadisticas-de-produccion/, Accessed date: 17 January 2017.
Soto, C., 2010. Hidrogeología e Hidroquímica de Aguas Sugterráneas en el Distrito Inca de Oro, Región de Atacama: Procesos de Interacción Agua-Roca y Dispersión Geoquímica (Tesis Para Optar al Grado de Magíster en Ciencias Mención Geología). Universidad de Chile, Santiago.
Stern, C.R., 2004. Active Andean volcanism: its geologic and tectonic setting. Rev. Geol. Chile 31, 161–206. http://dx.doi.org/10.4067/S0716-02082004000200001.
Tapia, J., Audry, S., 2013. Control of early diagenesis processes on trace metal (Cu, Zn, Cd, Pb and U) and metalloid (As, Sb) behaviors in mining- and smelting-impacted lacustrine environments of the Bolivian Altiplano. Appl. Geochem. 31, 60–78. http://dx.doi.org/10.1016/j.apgeochem.2012.12.006.
Tapia, J., Verdejo, F., 2015. Metal(loid)s distribution in northern Atacama Region hydrological basins. In: Presented at the 27th International Applied Geochemistry Symposium, Tucson, Estados Unidos.
Tapia, J., Audry, S., Townley, B., Duprey, J.L., 2012. Geochemical background, baseline and origin of contaminants from sediments in the mining-impacted Altiplano and Eastern Cordillera of Oruro, Bolivia. Geochem. Explor. Environ. Anal. 12, 3–20. http://dx.doi.org/10.1144/1467-7873/10-RA-049.
The World Bank, 2017. Mongolia | Data https://data.worldbank.org (web archive link, 2017). https://data.worldbank.org/country/mongolia, Accessed date: 4 October 2017.
Thompson, M., Palma, B., Knowless, J., Holbrook, M., 2003. Multi-annual climate in Parque Nacional Pan de Azúcar, Atacama Desert, Chile. Rev. Chil. Hist. Nat. 76, 235–254.
US EPA, 2009. Drinking WATER Contaminants. WWW Document. http://water.epa.gov/drink/contaminants/, Accessed date: 26 January 2015.
Valero-Garcés, B.L., Delgado-Huertas, A., Navas, A., Edwards, L., Schwalb, A., Ratto, N., 2003. Patterns of regional hydrological variability in central-southern Altiplano (18°–26°S) lakes during the last 500 years. Palaeogeogr. Palaeoclimatol. Palaeoecol. 194, 319–338. Late-quaternary palaeoclimates of the southern tropical Andes and adjacent regions. https://doi.org/10.1016/S0031-0182(03)00284-0.
Vargas, G., Ortlieb, L., Rutllant, J., 2000. Aluviones históricos en Antofagasta y su relación con eventos El Niño/Oscilación del Sur. Rev. Geol. Chile 27, 157–176. http://dx.doi.org/10.4067/S0716-02082000000200002.
Weather Online, 2017. Climate of the World: Iran | weatheronline.co.uk (web archive link, 2017). http://www.weatheronline.co.uk/reports/climate/Iran.htm, Accessed date: 5 October 2017.
White, N., Hedenquist, J.W., 1995. Epithermal gold deposits styles, characteristics and exploration. SEG Newsl. 23, 9–13.
WHO, 2011. WHO|Guidelines for Drinking-Water Quality, fourth edition. WHO, URL WWW Document. http://www.who.int/water_sanitation_health/publications/2011/dwq_guidelines/en/, Accessed date: 27 January 2015.
Wilcox, A.C., Escauriaza, C., Agredano, R., Mignot, E., Zuazo, V., Otárola, S., Castro, L., Gironás, J., Cienfuegos, R., Mao, L., 2016. An integrated analysis of the March 2015 Atacama floods. Geophys. Res. Lett. 43, 2016. (GL069751). https://doi.org/10.1002/2016GL069751.
Zhang, J., Liu, C.L., 2002. Riverine composition and estuarine geochemistry of particulate metals in China—weathering features, anthropogenic impact and chemical fluxes. Estuar. Coast. Shelf Sci. 54, 1051–1070. http://dx.doi.org/10.1006/ecss.2001.0879.
Zoller, W.H., Gladney, E.S., Duce, R.A., 1974. Atmospheric concentrations and sources of trace metals at the south pole. Science 183, 198–200. http://dx.doi.org/10.1126/science.183.4121.198.